UC San Diego
UC San Diego Electronic Theses and Dissertations

Title

Characterizing regulation of PNKP activity by Fru-2,6-P2 and IKK2

Permalink

https://escholarship.org/uc/item/4rf99152

Author

Huai, Weihan

Publication Date

2022

Peer reviewed|Thesis/dissertation

UNIVERSITY OF CALIFORNIA SAN DIEGO

Characterizing regulation of PNKP activity by Fru-2,6-P$_2$ and IKK2

A Thesis submitted in partial satisfaction of the requirements

for the degree Master of Science

in

Chemistry

by

Weihan Huai

Committee in charge:

Professor Gourisankar Ghosh, Chair

Professor Patricia Jennings

Professor Simpson Joseph

2022

The Thesis of Weihan Huai is approved, and it is acceptable in quality and form for publication on microfilm and electronically.

University of California San Diego

2022

DEDICATION

This Thesis is dedicated to my father, Xiaoming Huai, who supports me during my study in the US and cheered me up when I was in the bottom.

TABLE OF CONTENTS

LIST OF FIGURES

LIST OF TABLES

ACKNOWLEDGEMENTS

I would like to give my thanks to all the people who helped me throughout my study. First, I would like to thank my father, Xiaoming Huai, for his support and encouragement to my study. I would also like to give my thank to Professor Gourisankar Ghosh for providing me the opportunity to work on this fascinating project. Furthermore, I would like to thank all current and former members of Gourisankar Ghosh Lab who provided help on my study, including Dr Tapan Biswas, Dr. Kaushik Saha, Shandy Shahabi, Myung Soo Ko, Dr. Suborno Jati. Finally, I would like to thank my collaborators, Dr. Tapas Hazra, and Dr. Anirban Chakraborty, for their help and cooperation on my project.

I acknowledge Dr. Anirban Chakraborty for conducting the radiolabeled phosphatase assay in figure 19 and the in vitro kinase assay on figure 18.

ABSTRACT OF THE THESIS

Characterizing Regulation of PNKP Activity by Fru-2,6-P$_2$ and IKK2

by

Weihan Huai

Master of Science in Chemistry

University of California San Diego, 2022

Professor Gourisankar Ghosh, Chair

Polynucleotide kinase/phosphatase (PNKP) is an essential enzyme for DNA repair, and its dysfunction is related to many neurological diseases. However, how PNKP is regulated in nucleus is not fully understood yet. Our collaborator found that the metabolic enzyme 6-phosphofructokinase/fructose-2,6-biphosphatase 3 (PFKFB3) is a component of the PNKP-associated DNA repair complex. Since the major role of PFKFB3 is to produce Fru-2,6-P$_2$, we

hypothesized that Fru-2,6-P$_2$ plays an important role in DNA repairing. I prepared and purified Fru-2,6-P$_2$ in in vitro, and used both biochemical assay and binding experiments to show that Fru-2,6-P$_2$ enhanced PNKP activity in vitro through direct binding. Moreover, I found that PNKP is phosphorylated by IκB Kinase 2 (IKK2) in vitro. Furthermore, I tested Fru-2,6-P$_2$ level in spinocerebellar ataxia 3 (SCA3) patients and Huntington Disease patient samples (postmortem brains), and found that the Fru-2,6-P$_2$ levels are lower in all SCA3 and most HD patient samples tested. Our results elucidate the significance of Fru-2,6-P$_2$ and PFKFB3 in DNA repair and suggest that Fru-2,6-P$_2$ plays an important role in many neurological diseases. Furthermore, in vitro studies on IKK2 phosphorylating PNKP indicates that IKK2 is a possible regulator of PNKP.

I.   Introduction

Oxidative stress, DNA damage, and neurological diseases

Brains are thought to metabolize one-fifth of the consumed oxygen, making it extremely vulnerable to oxidative stress (Madabhushi, 2014). The oxidative stress is induced by the production of the reactive oxygen species (ROS), which is produced during oxidative phosphorylation in mitochondria. Exposure to ROS renders the genomic and mitochondrial DNA susceptible to DNA damage. A robust DNA repairing system is required for maintaining the integrity of the genome. The accumulation of DNA damage has been observed in many neurological diseases such as Parkinson's disease (PD), Alzheimer's disease (AD), and amyotrophic lateral sclerosis (ALS) (Bender et al., 2006; Mullaart et al., 1990; Martin, 2001). Repairing oxidative damage requires the assembly of DNA repairing complex involving Huntington (HTT) and Ataxin-3 (ATXN3) proteins, which have distinctive functions during the DNA repair. Pathogenic forms of these proteins with expanded polyglutamine-rich segments fail to perform their normal functions, which disrupts DNA repair and eventually leads to Huntington disease (HD) and Spinocerebellar ataxia type 3 (SCA3) (Gao, et al., 2019; Chakraborty et al., 2020). More specifically, the histone acetylase, Creb Binding Protein (CBP), undergoes degradation in brains expressing mutant HTT (mHTT) in the case of HD (Jiang et al., 2003). In the case of SCA3, RNA polymerase II is degraded by the actions of mATXN-3 (Chakraborty et al., 2020). Interestingly, overexpression of PNKP, an essential DNA repairing enzyme, in Drosophila expressing mutant ATXN3 ameliorates the SCA3 pathogenic phenotype, indicating the importance of PNKP in these neurological disorders (Chakraborty et al., 2020).

DNA repair and PNKP

DNA damage consists of unwanted base modification, base loss, and strand breaks, and plays a significant role in aging, cancer, and neurological diseases. The strand break can be

induced by a large variety of factors, including reactive oxygen species (ROS), ionization irradiation (IR), and cytotoxic agents. These factors induce strand breaks with different mechanisms and result in different termini. To counter the strand breaks and other DNA damages, cells have developed sophisticated repair pathways, and these pathways require a 5'-phosphate and 3'-OH termini for the ligation of broken strands, which means that unwanted termini must be modified before ligation.

The most common end termini product of single and double-stranded DNA is 3'-phosphate. To remove the phosphate from the 3' end, polynucleotide kinase/phosphatase (PNKP) is required. PNKP is a critical bifunctional end processing enzyme involved in DNA damage repair. It is responsible to remove the phosphate on the 3'end of the broken DNA and phosphorylates 5'-OH termini, which makes broken DNA compatible for ligation or elongation. The 3' phosphatase activity of PNKP is much higher than the 5' kinase activity, and studies showed that the 3' phosphatase activity takes precedence when both the 3'-phosphate and 5'-OH present (Dobson et al., 2006).

PNKP consists of 3 domains: A N-terminal fork-head associated (FHA) binding domain which is responsible for binding with either phosphorylated XRCC1 or XRCC4 to recruit the protein into the DNA repairing complex in different DNA repair pathways, and a phosphatase domain which dephosphorylates 3' phosphate on the broken DNA 3'-termini, and a C-terminal kinase domain which phosphorylates 5' hydroxyl group. The phosphatase activity of PNKP requires an Mg^{2+} cofactor. (Graces, et al., 2011) PNKP participates in a broad range of DNA repair pathways, including single strand break repair (SSBR), base excision repair (BER), and double-strand base repair (DSBR), due to the wide presence of 3'-phosphate during the DNA damage and repair. In SSBR, phosphorylated XRCC1 recruits PNKP into the DNA repairing

complex and works with DNA ligase to repair the broken DNA. In BER, PNKP is responsible for the removal of 3'-phosphate produced by cleaving the abasic sites. The DSBR undergoes two independent pathways: homologous recombination (HR) in replicating cells or non-homologous end-joining (NHEJ) in dividing/non-dividing cells. The PNKP is recruited to the DNA repairing complex by phosphorylated XRCC4 in the classical NHEJ pathway (c-NHEJ), which uses Ku, DNA-PK, 53BP1, and XRCC4/Lig-IV to repair broken DNA double-strand. (Figure 1)

Current studies on PNKP focus mostly on neurological disorders caused by PNKP mutations. Mutations in PNKP can cause many neurological diseases, including microcephaly with seizures (MCSZ) and ataxia with oculomotor apraxia type 4 (AOA4) (Dumitrache et al., 2016). The regulation of PNKP activity by factors other than XRCC proteins, however, is still unclear, while there have been studies that identified factors that regulate PNKP activity through protein modification. For instance, research has shown that ATM can phosphorylate PNKP to prevent it from ubiquitination and further proteasome degradation (Parsons et al. 2012). There is still a long way to understand how the regulation of PNKP in cells worked as well as their molecular basis.
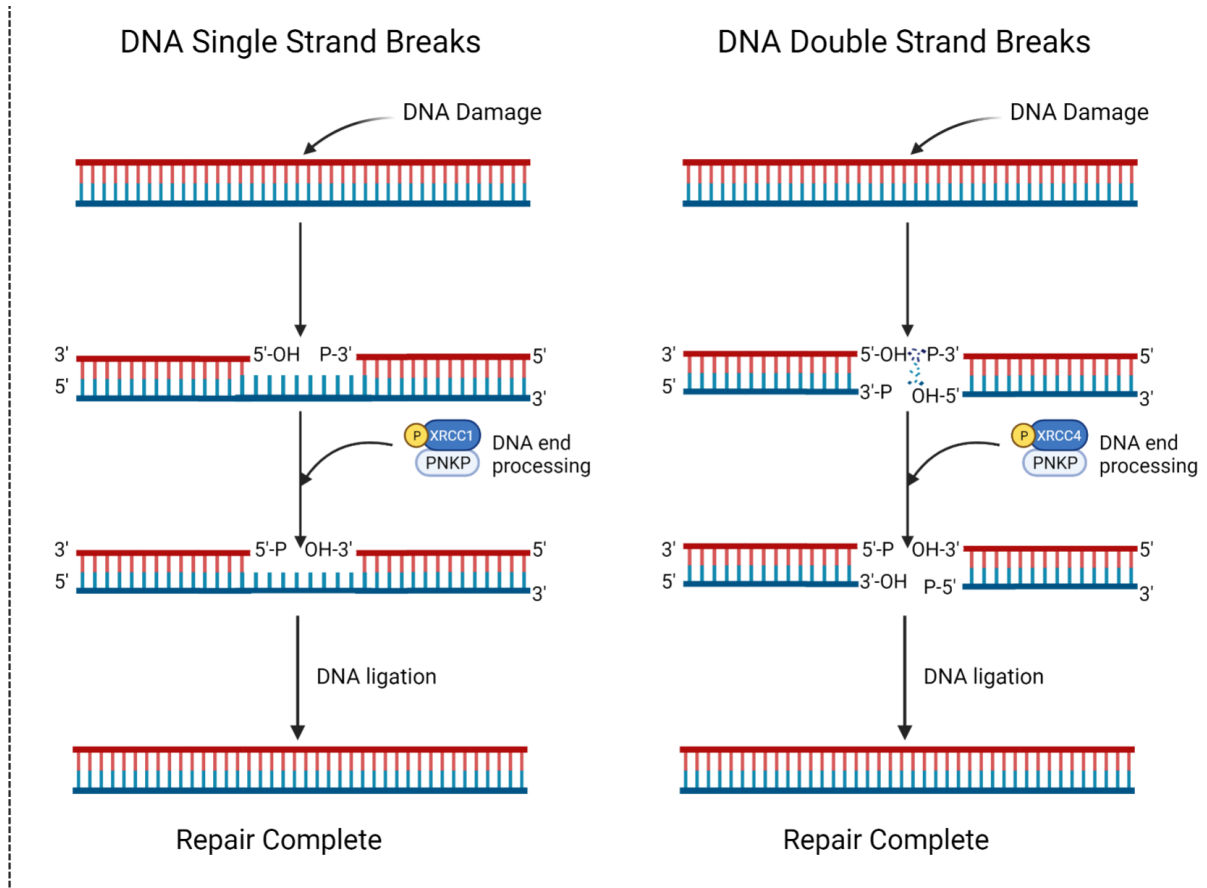
Figure 1: Role of PNKP in DNA single-strand and double-strand break repair.

IKK2

NF-κB signaling pathway is one of the major pathways activated in response to different stimuli which lead to the activation of genes responsible for cytokine production and cell survival. In a quiescent state, NF-κB proteins are bound to IκB (inhibitor of NF-κB) proteins and stay in the cytoplasm. Upon the canonical NF-κB activation, IκB proteins are phosphorylated and degraded, and the released NF-κB proteins enter the nucleus and bind to the NF-κB binding sites on genes to activate specific genes (Karin et al., 2000).

The phosphorylation of IκB proteins is performed by the IKK complex, which consists of three proteins: IKKα(IKK1), IKKβ(IKK2), and NEMO. The IκB kinase β, usually written as IKKβ or IKK2, is a master regulator of cell inflammatory response. It is a serine/threonine class of protein kinase that functions as an important upstream regulator of the NF-kB pathway. Upon activation by upstream signals such as TNF-α, IKK2 forms a complex with IKK1 and NEMO and gets activated. The activation of IKK2 requires the autophosphorylation at residues Ser177 and Ser181 on its activation loop (Delhase, et al., 1999). In unstimulated cells, IKK2 remains unphosphorylated. Stimulation of cells will trigger the phosphorylation of IKK2 on two serine residues and activate it. Despite numerous studies since its discovery, the mechanism of how IKK2 is phosphorylated and activated remains unanswered.

The most well-documented role of IKK2 is its activation of the canonical NF-kB signaling pathway. In the canonical NF-κB signaling pathway, it forms a multi-subunit complex with IKK1 and NEMO and phosphorylates IkBα on Ser32 and Ser36, which induces subsequent IkBα polyubiquitination and degradation and the translocation of released NF-κB dimers into the nucleus. In addition to the canonical NF-kB activation pathways, IKK2 also phosphorylates other

molecules in the NF-κB pathway. For instance, IKK2 phosphorylates RelA/p65 at Ser536, which enhances NF-κB activity (Yang et al., 2003). Besides, IKK2 phosphorylates NF-kB family member p105 and induces its polyubiquitination and degradation like IkBα. While p105 involves not only in the NF-κB pathway but also in other signaling pathways such as the TPL-2 pathway, activation of IKK2 will also lead to the activation of respective pathways. (Beinke et al., 2004)

Besides its role in NF-κB signaling, IKK2 can also phosphorylate other substrates than NF-κB proteins and is involved in other cellular functions. For example, IKK2 can phosphorylate the Forkhead transcription factor FOXO3a, a tumor suppressor protein that induces apoptosis (Hu et al., 2004). To date, IKK2 has been found to play a role in a variety of biological functions independent of NF-κB, as shown in Figure 2. This phenomenon also applies to IKK1 and other atypical IKK proteins such as TBK1 and IKKε, which phosphorylate novel NF-κB independent substrates, leading to various cellular outcomes (Antonia, et al., 2021). Given the significance of IKK2 in a wide variety of diseases including cancer, diabetes, and autoimmune disorders, it is important to understand the ability of IKK proteins to phosphorylate these novel substrates.

The IKK2 consensus phosphorylation motif has not been fully established yet. The "DpSGΨXpS/T" sequence that highlights a pair of serines is found in many IKK2 substrates in the canonical NF-κB pathway such as IκB proteins but not in all substrates (Chariot 2009). While this motif is not highly conserved among IKK2 substrates, especially for amino acids between two serine residues, which residues in the motif are essential for the IKK2 recognition is yet to be answered.
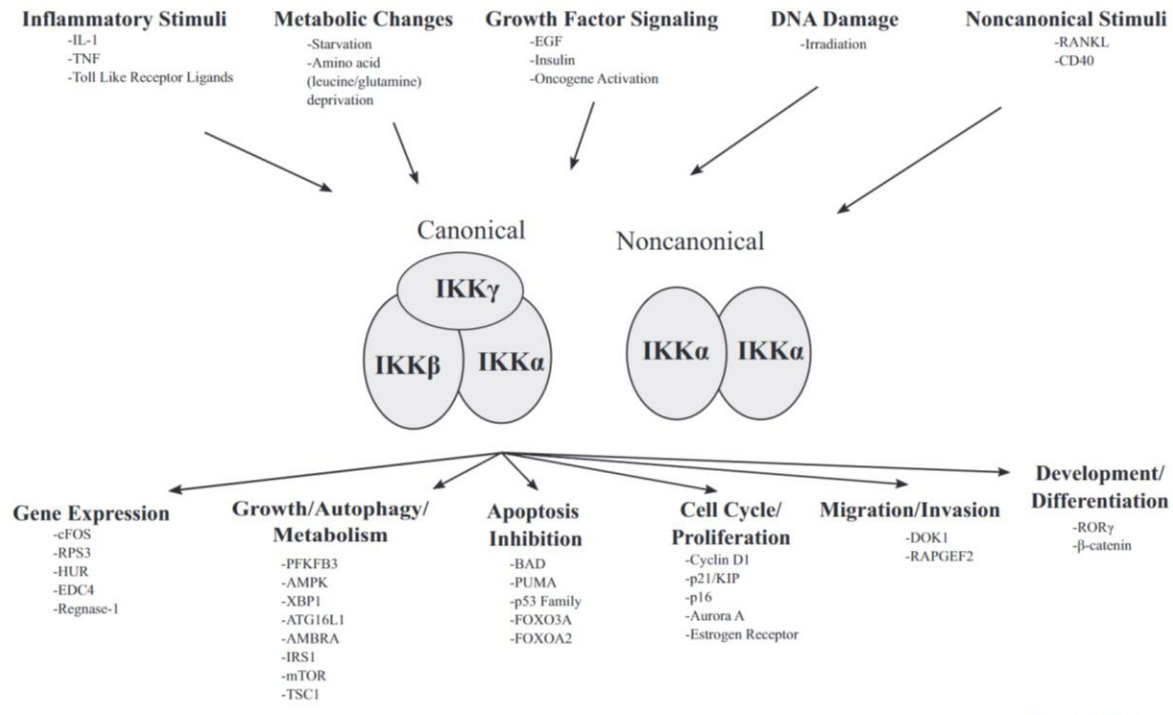
Figure 2: IKK complexes regulate a wide range of cellular processes. (Antonia et al., 2021)

Figure 3: Sequence homology of IKK2 substrates and phosphorylation sites. The highly conserved serine is shaded in yellow. (Schmid and Birbach, 2008)

PFK2, PFKFB3, and Fru-2,6-P$_2$

Fructose 2,6-bisphosphate (Fru-2,6-P$_2$) is an important metabolite known for its involvement in glucose metabolism. It activates (PFK-1), the rate determining enzyme of the multi-step glycolysis pathway. It allosterically activates PFK-1 by increasing its affinity to its substrate fructose 6-phosphate, while decreasing its affinity to inhibitors such as citrate. PFK-1 converts fructose 6-phosphate (F6P) into fructose 1,6-bisphosphate (Fru-1,6-P$_2$), which is the rate-limiting step in glycolysis (Hers and Schaftingen, 1982).

The production and degradation of Fru-2,6-P$_2$ are performed by the bifunctional enzyme phosphofructokinase-2/fructose biphosphotase-2 (PFK-2/FBPase-2) (Pilkis et al., 1995). In humans, PFK-2/FBPase-2 is encoded by four genes (PFKFB1-4). These four isozymes have distinct properties such as the kinase/phosphatase activity ratio, and tissue expression profile, and can be involved in different pathways (El-Maghrabi et al., 2001). Among all four isozymes, PFKFB3 shows unique properties: it has the highest kinase/phosphatase ratio (740:1) (Okar et al., 2001). It is also the only inducible PFKFB isozymes that can be regulated by many factors such as stress stimuli, hypoxia, and growth factors. Furthermore, PFKFB3 is the only isozyme that can be trafficked into the nucleus (Yalcin et al., 2009). Besides its role in regulating glycolysis, PFKFB3 also has other cellular functions. For instance, it can activate cyclin-dependent kinase through Fru-2,6-P$_2$, which promotes cell progression and prevents apoptosis (Yalcin et al., 2009; Yalcin et al., 2014). Also, research showed that PFKFB3 played a role in the homologous recombination (HR) DNA repair pathway by recruiting RRM2 into the repairing foci to promote nucleotide incorporation, indicating that PFKFB3 plays a role in DNA repair (Gustafsson et al., 2018). However, the mechanism of how PFKFB3 and Fru-2,6-P$_2$ regulate the HR pathway is unclear.

Cancer cells usually maintain high glycolytic flux to sustain their growth, which was described by Otto Warburg and is now known as the "Warburg Effect" (Warburg et al, 1927). PFKFB3 has been a hot topic for its role in various tumor cells since its expression is found elevated in several cancers (Atsumi et al., 2002). As one of the regulators of glycolytic flux, it is closely associated with cancer growth. Extensive studies focused on the role of PFKFB3 in cancers as well as the development of small inhibitors of PFKFB3. To date, there are three well-characterized inhibitors of PFKFB3, and their effect on cancer is still on the way.
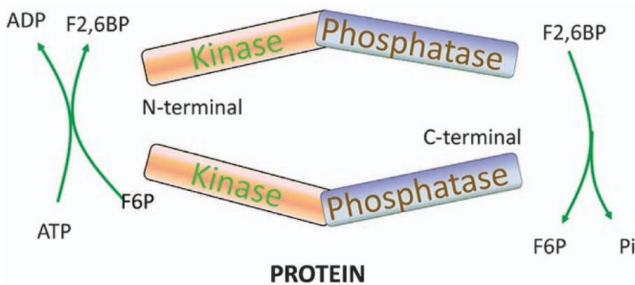
Figure 4: Schematic kinase and phosphatase functions of PFKFB3. (Shi, et al., 2017)
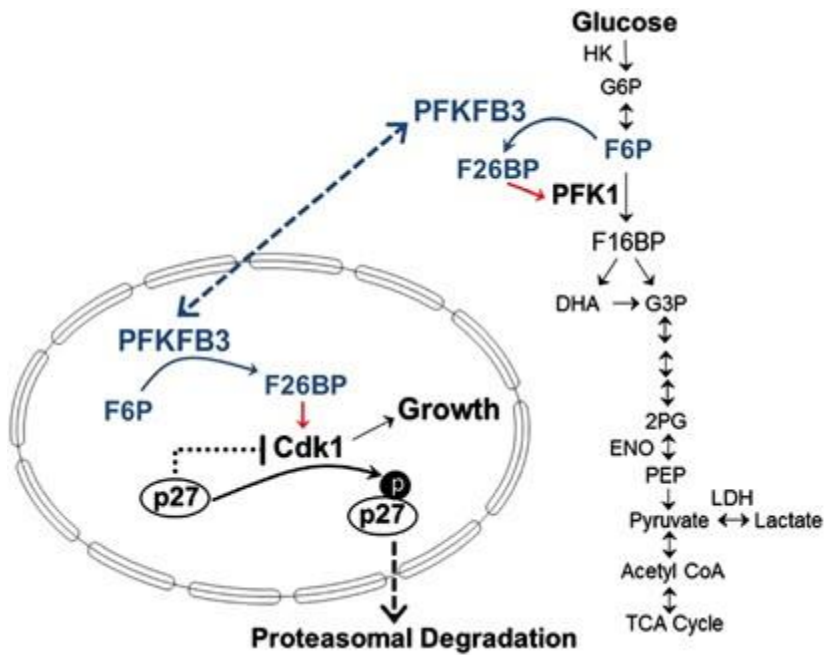
Figure 5: Role of PFKFB3 in glycolysis and cell survival. In cytoplasm, PFKFB3 produces

Fru-2,6-P_2 and stimulates glycolysis. In nucleus, one of the known functions of PFKFB3 is its

role on regulating Cdk1 activity and p27 degradation. (Yalcin et al., 2014)

Focus of my study:

My project starts with the study of PNKP functions in neurodegenerative diseases. Our collaborators found that PFKFB3 is involved in the PNKP-associated DNA repair complex, and PNKP activity is impaired in the PFKFB3 depleted cells. However, the in vitro phosphatase assay showed that PFKFB3 alone does not enhance PNKP phosphatase activity, while the activity is enhanced with further addition of F6P. Therefore, we purposed that the product of PFKFB3, Fru-2,6-P_2, directly binds to PNKP and enhances its phosphatase activity. Therefore, the first part of my project is to understand how Fru-2,6-P_2 modulate PNKP activity. My goal is to prepare and purify Fru-2,6-P_2 in large quantity, and characterize its interaction with PNKP. Also, I study how Fru-2,6-P_2 affects PNKP activity using a biochemical assay system.

Besides my study of Fru-2,6-P_2 on PNKP, we found a motif in PNKP sequence that is close to the IKK2 phosphorylation motif, and we purposed that the IKK2 is a possible upstream regulator of PNKP which phosphorylates Ser280 and Ser284 on PNKP. The second part of my project is to demonstrate the phosphorylation of PNKP by IKK2, and how the phosphorylation modulates PNKP activity. Finally, I aimed to measure the level of Fru-2,6-P_2 in brains of SCA3 and HD patients to characterize the significance of Fru-2,6-P_2 in neurodegenerative diseases.

II.   Materials and Methods

A. Cloning of PNKP and Site-directed mutagenesis

1. Cloning His-tagged PNKP and mutants

PCR fragments of the PNKP construct were amplified from the plasmid obtained from our collaborator using the pfu I enzyme. PNKP constructs were cloned into pET28a with BamHI and NdeI endonucleases.

Mutant PNKP, including PNKP S284A, PNKP S284E, PNKP S280E, PNKP S280E/S284E, PNKP S284C, PNKP S284T, PNKP S280A, and PNKP S280E/S284C, were cloned using point-directed mutagenesis method with the Pet28a-PNKP template. The template plasmid was digested using DpnI endonuclease, and the clones were sequenced to ensure that the mutation is introduced.

2. Cloning of GST-tagged PNKP

For the cloning of GST-tagged PNKP, PNKP constructs were amplified from pET28a using the pfu I enzyme and cloned into pGEX-4T2 with BamHI and XhoI endonucleases.

B. Protein Purification Protocols

1. His-tagged PNKP and mutants

Proteins are expressed in BL21 Rosetta (DE3) *E.coli* cells. The 2 Liter LB culture was shaken at 37°C till the OD_{600} reaches 0.4. The culture was then induced with 0.2m M IPTG overnight at room temperature and centrifuged at 3000rpm at 4°C for 30 mins. The pellet is resuspended in chilled lysis buffer (25mM Tris-HCl pH7.5, 500mM sodium chloride, 10% glycerol, 5mM BME, 10mM imidazole, 0.1% NP-40, 0.1mM phenylmethylsulfonyl fluoride

(PMSF)). After dispensing the resuspended lysate into a steel beaker stored on packed ice, the lysate was then sonicated with 6 cycles using the following condition: 20 seconds on with 50% duty cycle and power setting 8 and 40 seconds off. The lysate was then centrifuged at 20000rpm for 30 minutes at 4°C. The supernatant was incubated with 2mL of equilibrated Ni-NTA resin with constant rotation for 2 hours at 4°C. The mixture was then spun down at 3000rpm for 3 minutes at 4°C, and the supernatant is removed. The beads were then washed two times with 50mL of wash buffer (lysis buffer without PMSF+ 10mM imidazole) and eluted with a cold elution buffer (wash buffer +240mM imidazole) in a series of 1mL elution fractions. The elutes were then loaded onto a Superdex-75 size exclusion column and eluted with the gel filtration buffer (25mM Tris-HCl pH7.5, 500mM sodium chloride, 5% glycerol, 1mM DTT). The peak fractions were collected and concentrated using polyethylene glycol (MW 20000).

All the PNKP mutant proteins (S280E, S280A, S280C, S284E, S284A, S284C, S284T, EE, EC) were purified in the way described above.

2. Purification of GST-PNKP

GST-PNKP was expressed in BL21 Rosetta (DE3) *E. coli* cells. The 2 Liter LB culture was shaken at 37°C and was induced with 0.2mM IPTG overnight at 16°C at OD_{600}=0.3 and centrifuged at 3000rpm at 4°C for 30 mins. The pellet is resuspended in chilled lysis buffer (25m M Tris-HCl pH7.5, 150m M sodium chloride, 0.1mM magnesium chloride, 10% glycerol, 1mM DTT, 0.5mM PMSF). The lysates were sonicated with 5 cycles using the following condition: 20 seconds on, 40 seconds off, 50% duty cycle, and power setting 7. The lysate was then centrifuged at 20000rpm for 30 minutes at 4 °C. The supernatants were then incubated with 1mL of pre-equilibrated glutathione agarose resin and incubated with constant rotation for 2 hours at 4°C. The mixture was then spun down at 500x g for 3 minutes at 4°C, and the supernatant is

removed. The beads were then washed two times with 50mL of wash buffer (same as lysis buffer without PMSF), and eluted stepwise with 1mL per step by elution buffer (wash buffer + 10mM reduced glutathione). The eluted samples were analyzed on SDS-PAGE gel and Elute 1 was dialyzed with 500mL of dialysis buffer (wash buffer without $MgCl_2$).

3. Purification of His-PFKFB3

His-PFKFB3 was expressed in BL21 pLysS *E. coli* cells. The 2 Liter LB culture was shaken at 37°C and was induced with 0.2mM IPTG at 37°C for 3 hours at OD_{600}=0.4 and centrifuged at 3000rpm at 4°C for 30 mins. The pellet is resuspended in chilled lysis buffer (25mM Tris-HCl pH7.5, 300mM KCl, 10% glycerol, 10mM imidazole, 0.1% NP-40, 0.1mM PMSF). After dispensing the resuspended lysate into a steel beaker stored on packed ice, the lysate was then sonicated with 5 cycles using the following condition: 20 seconds on with 50% duty cycle and power setting 6 and 40 seconds off. The lysate was then centrifuged at 20000rpm for 30 minutes at 4°C. The supernatant was incubated with 2mL of equilibrated Ni-NTA resin with constant rotation for 2 hours at 4°C. The mixture was then spun down at 3000rpm for 3 minutes at 4°C, and the supernatant is removed. The beads were then washed two times with 50mL of wash buffer (lysis buffer without PMSF + 10mM imidazole) and eluted with a cold elution buffer (wash buffer +240m M imidazole) in a series of 1mL elution fractions. The first three fractions were collected and concentrated with polyethylene glycol (MW 20000) to a final concentration of 3mg/mL.

4. Purifying PPi-PFK

Pyrophosphate-dependent phosphotransferase (PPi-PFK) is purified from potato tubers using the protocol developed by Schaftingen et al. (Schaftingen et al, 1982). 300g of potato

tubers are homogenized in a Waring blender with 2 volumes of lysis buffer (20mM HEPES pH8.2, 20mM potassium acetate, 2mM DTT). The mixture was filtered through a cheesecloth. Solid sodium pyrophosphate and 1M $MgCl_2$ were then added to the filtrate to reach 2mM, and the pH is adjusted to 8.2. Next, the filtrate was heated in a 70°C water bath to 59°C and maintained for 5 mins at a 59°C water bath. The filtrate was then cooled down to 0°C and the pH is adjusted to 7.1. For every 100mL of the mixture, 6g of poly(ethylene glycol) (PEG) 6000 was added and mixed for 15 mins. The mixture is then allowed to stand for 10 mins and centrifuged for 15 mins at 4000x g. The pellet is discarded, and 8g of PEG 6000 was then added to every 100mL resulting supernatant and the sample was mixed for 5 mins. The mixture is then stood for 10 mins and centrifuged at 4000xg, and the supernatant is discarded. The pellet is dissolved in 40mL of buffer containing 20mM Tris-HCl pH8.2, 20mM KCl, and 2mM DTT and applied to 3mL of Q Sepharose Fast Flow resin. The column is washed with the same buffer with 60mM KCl and eluted with 30mL of buffer with 150mM KCl. The elute is diluted to 30mM KCl and passed through 1mL Q Sepharose Fast Flow resin and eluted again with 10mL buffer with 150mM KCl.

The activity of PPi-PFK was tested by the production of Fru-1,6-P_2. The PPi-PFK is mixed with a mixture of: 25mM Tris-HCl pH8.0, 5mM $MgCl_2$, 0.2mM NADH, 50µg/mL aldolase, 1µg/mL triosephosphate isomerase (TPI), 10µg/mL glycerol-3-phosphate dehydrogenase (GDH), an estimated 1µM Fru-2,6-P_2 to a total of 500µL. The reaction is initiated using 50µL 25mM sodium pyrophosphate, and the change in A_{340} is measured.

C. In-vitro pull-down assay

The binding buffer used in the in-vitro pull-down assay was composed of 150mM sodium chloride, 25mM Tris-HCl pH=7.5, 5% glycerol, 0.1% NP-40, 1mM DTT and was chilled on ice.

15μL of Glutathione resins are used for each reaction. Beads are washed with 200μL of binding buffer and spun down at 1000x g for 30 seconds, and supernatants are removed. 2μg of GST or GST-PNKP are added with 200μL of binding buffer. The mixtures were rotated at 4°C for 30 mins. The mixtures were then washed once with 500μL of binding buffer, and the supernatants were discarded. The beads were then resuspended with 200μL of binding buffer, and 4μg of his-tagged IKK2 was added to each mixture. The mixtures were then rotated at 4°C for 60 mins, spun down, and washed three times with 400μL of wash buffer. After the final wash, 4x SDS loading dye was added to the mixture to 1x, and beads were boiled on a heat block for 5 mins. Then, the beads were loaded to the SDS-PAGE gel and run at 200 volts for 45 mins, and a western blot was performed to visualize the result.

D. Western Blotting

The samples were run on 10% SDS-PAGE gel at 200 volts for 45 mins. To transfer the protein to the nitrocellulose membrane, the membrane, gel, foam pads, and blotting papers were rinsed with transfer buffer (25mM Tris, 192mM glycine, 10% methanol) for 1 min and packed as a transfer sandwich. The sandwich was then transferred to a tank between electrodes and ran at a constant current of 400mA for 100 mins. After the transfer, the nitrocellulose membrane was transferred to a clean cassette and blocked with 10mL of 5% milk in 1x TBST at room temperature for 1 hour. The membrane was then incubated with 10mL of 1:2000 diluted anti-His primary antibody in 1x TBST overnight at 4°C. The primary antibody was poured off and the nitrocellulose membrane was washed for 10 minutes three times with 1x TBST. 10mL 1:10000

diluted secondary antibody in 1x TBST was then added to the cassette and the membrane was incubated at room temperature for 1 hour, and the membrane was subsequently washed for 10 minutes three times with 1x TBST. The membrane was developed with 2mL of ECL buffer (10mM Tris-HCl pH8.6 with the addition of 4.4μL of p-coumaric acid, 10μL of luminol, and 1.5μL of hydrogen peroxide) and gently shaken for 90 seconds. The membrane was then dried and exposed in ChemiDoc with the same setting (60 images between 1 sec to 150 sec).

E. In vitro kinase assay protocol

1-2 μg of wild-type or mutant PNKP was used for each reaction mixture. Proteins were incubated with kinase buffer (20mM Tris-HCl pH 7.5, 100mM sodium chloride, 10mM $MgCl_2$, 1mL DTT, 200μM ATP). ^{23}P-labeled ATP and 50ng of IKK2 were added to initiate the reaction, and the mixture was incubated for 30 mins. The reaction was terminated by adding 4x SDS loading dye and boiling on heat-block for 5 mins, and samples were loaded on 12.5% SDS-PAGE gel and run for 45 mins at 200V. The front band of the gel was removed by razor, and the gel was wrapped with saran wrap. The gel was then incubated with a pre-blanked phosphor screen in darkness overnight. The next day, the screen was analyzed on the Tycoon FLA9000 phosphorimager to visualize radioactive bands.

F. Protocol for preparing Fru-2,6-P_2

1. Purification using the batch method:

2μL of 50mM fructose-6-phosphate was used for each reaction. 10 reactions were performed in parallel. A reaction cocktail consisting of 60mM Tris-HCl (pH 7.5), 1.5mM DTT, 5mM KP_i (pH 7.5), 20mM KCl, 40μM EDTA, 6mM $MgCl_2$, 5mM ATP, 10% glycerol, 1mg/mL BSA (Buffer B) was then added to the reaction to a final volume of 200μL. The reaction was initiated

19

by adding 100μg of PFKFB3. The reaction mixtures were incubated at 37°C for 90 mins. The reaction was quenched by incubating at 80°C for 5 mins to inactivate enzymes. Each reaction sample was spun down at 12000rpm for 1 min and diluted with 2mL using 10mM TEABC (pH 8.5) and all the samples were pooled together. Next, the sample was applied to 1.5mL of Q Sepharose Fast Flow beads pre-equilibrated with 10mM TEABC (pH 8.5). The resin was step eluted with TEABC buffer (pH8.5, 100-500mM, 50mM/step, 3mL/step), and the fraction with 350mM TEABC was collected and stored at -20°C, and 1mL of the fraction was sent to the Mass spec facility to check the presence of Fru-2,6-P_2. The rest of the fraction was evaporated to dryness using the Savant SpeedVac, and the solid was dissolved into 20mM Tris-HCl (pH8.0). Negative control was prepared in the same way despite that the PFKFB3 was inactivated by incubating on a 95°C heat block for 5 mins before initiating the reaction. The 350mM TEABC fraction was evaporated and dissolved into 20mM Tris-HCl (pH8.0).

2. Purification using Mono Q 5/50 GL

The 350mM fraction solids obtained from the previous batch step were dissolved in 1mL of 10mM TEABC pH8.5 and injected into the Mono Q 5/50 GL column. Then the column is eluted with the gradient (Buffer A: 10mM TEABC pH8.5, Buffer B: 800mM TEABC pH8.5, 10mL 0-32% B, 20mL constant 32% B, 10mL 32-80% B, 4mL 100% B). the fractions were collected and tested for the presence of Fru-2,6-P_2 using the PPi-PFK assay.

3. Purification using prepacked Q Sepharose Fast Flow

The production of Fru-2,6-P_2 is performed with the same method described above. After the reaction is quenched, the sample was diluted with 10 volumes of 10mM TEABC pH8.5 and injected into a prepacked 5mL Q Sepharose Fast Flow column. Fru-2,6-P_2 was eluted using the

gradient (Buffer A: 10mM TEABC pH8.5, Buffer B: 800mM TEABC pH8.5, 15mL 0-32% B, 12mL constant 32% B, 10mL 32-80% B, 4mL 100% B). All fractions were tested using the PPi-PFK assay and fractions containing Fru-2,6-P_2 was evaporated to dryness using the Savant SpeedVac.

G. Fru-2,6-P_2 measurement

Measurement of Fru-2,6-P_2 is performed using the method developed by Schaftingen et al. using pyrophosphate-dependent phosphotransferase (PPi-PFK), aldolase, triose phosphoisomerase (TPI), and glycerol-3-phosphate dehydrogenase (GDH) (Schaftingen at al. 1982). The 450µL enzymatic mixture containing 25mM Tris-HCl pH 8, 0.2mM NADH, 5mM $MgCl_2$, 5mM F6P, 0.01U PPi-PFK, 50µg/mL aldolase, 1µg/mL TPI, 10µg/mL GDH, and purified Fru-2,6-P_2 is initiated by adding 50µL of 25mM sodium pyrophosphate, and the reaction is incubated at room temperature for 10 mins. The reaction is quenched by adding 55µL of 10% SDS, and the change in A_{340} is measured. To accurately quantify Fru-2,6-P_2, a large scale of Fru-2,6-P_2 is converted to F6P by adding 0.1M HCl, and the mixture is incubated at 37°C for 30 mins. The reaction is quenched by adding an equivalent amount of 0.1M NaOH, and the increase in F6P is measured using the F6P assay kit (Sigma Aldrich). The measured Fru-2,6-P_2 was then diluted to the nM scale and the change of A_{340} was measured to construct a linear standard curve. The Fru-2,6-P_2 from purification and cortex samples were diluted until the change of A_{340} falls into the standard curve range.

H. Characterizing PNKP stability change

Fru-2,6-P$_2$ purified from the prepacked Q Sepharose Fast Flow was dissolved into 10μL

of buffer containing 25mM Tris-HCl pH7.5, 150mM NaCl, 5mM MgCl$_2$, 1% glycerol, and 1mM

DTT, and the concentration was measured by PPi-PFK assay before the experiment. WT PNKP

was diluted with the same buffer to 0.3mg/mL, and dissolved Fru-2,6-P$_2$ with corresponding

concentration (18.75-150μM) were mixed with diluted PNKP and loaded into TY-C001

capillaries at room temperature. Thermal denaturation was conducted on the NanoTemper Tycho

machine and the first derivative of A$_{350}$/A$_{330}$ was measured.

I. PNKP biochemical activity assay

The activity of PNKP is measured using a fluorescent-based biochemical activity assay.

The fluorophore-labeled deoxyribonucleotide substrates are the same as oligos used in *Kalasova*

et al., which are: [5'-(TAMN)-TAGCATCGATCAGTCCTC-3'-P], [5'-OH-

GAGGTCTAGCATCGTTAGTCA-(6-FAM)-3'], and the complementary strand [5'-

TGACTAACGATGCTAGACCTCTGAGGACTGATCGATGCTA-3']. (Kalasova et al., 2019)

To prepare the substrate for the assay, equimolar amounts of oligos are mixed in the annealing

buffer (10mM Tris-HCl pH7.5, 200mM NaCl, 1mM EDTA) and annealed by adding the

microtubes into the 700mL boiling water and let it freely cool down to room temperature. For the

assay, 0.1ng of purified PNKP is incubated with 50nM substrates in 50μL reaction buffer (25mM

Tris-HCl pH7.5, 130mM KCl, 10mM MgCl$_2$, 1mM DTT, 1mg/mL BSA) at 37°C for 30 mins.

The reaction is quenched by adding an equal amount of quenching buffer (90% formamide,

50mM EDTA, 0.1% bromophenol blue). The mixture is heated on a 95°C heat block for 5 mins,

and 6μL of the mixture is separated on a 20% Urea-PAGE gel. The TAMRA fluorescence is

detected using the Typhoon FLA 9000 laser scanner.

J. Microscale thermophoresis

Wild-type PNKP purified from the size exclusion column was firstly diluted to 10μM and labeled with fluorescent dye using the Protein Labelling Kit Red-NHS 2nd Generation (NanoTemper). For the binding experiment, fluorescence-labelled PNKP was diluted with the buffer containing Tris-HCl pH7.5, 150mM NaCl, 10mM $MgCl_2$, 0.05% Triton X-100, and 1mM DTT. Fru-2,6-P_2 purified using the Q Sepharose Fast Flow was dissolved with the same buffer and the concentration was determined using the PPi-PFK assay. Fru-2,6-P_2 with serial dilutions was mixed with the indicated protein and incubated in darkness for 20mins. Mixtures were loaded into MO-K025 capillaries at room temperature.

K. Measuring Fru-2,6-P_2 levels in patient cortex samples

The front cortex of healthy people and SCA3 or HD patients were received from our collaborators from UTMB. The PNKP activities of each patient's cortex tissues were tested by our collaborators. The Fru-2,6-P_2 level in the nuclear extract of samples was measured using the PPi-PFK assay. 10mg of tissues were used to prepare the nuclear extract. Tissues were resuspended with 5 tissue volumes of Buffer A (10mM HEPES pH7.4, 1.5mM $MgCl_2$, 10mM KCl, 0.5mM DTT, 1mM Na_3VO_4, 1mM PMSF, and 1:200 protease inhibitor cocktails), and 5 tissue volumes of Buffer B (10mM HEPES pH7.4, 1.5mM $MgCl_2$, 10mM KCl, 0.5% NP-40, 1:200 protease inhibitor cocktails) were added immediately. Tissues were homogenized immediately after buffer B was added. The homogenized samples were kept on ice for 10 mins. The samples were then spun down at 600 x g for 10 mins, and the supernatants were collected as the cytosolic fraction. The pellets were washed and spun down 3 times with 10 sample volumes of Buffer A. The washed pellets were resuspended in 10 tissue volumes of Buffer C (20mM HEPES pH7.4, 25% glycerol, 420mM NaCl, 1.5mM $MgCl_2$, 0.2mM EDTA, 0.5mM DTT, 1Mm

PMSF, 1mM Na_3VO_4, 1:200 protease inhibitor cocktails) and kept on ice for 1.5 hours with routinely tapping every 30 mins. The samples were then spun down at 12500 rpm for 15 minutes, and the supernatants were kept as the nuclear extracts. The concentration of Fru-2,6-P_2 in nuclear extracts was measured using the PPi-PFK assay as described above.

III.   Result
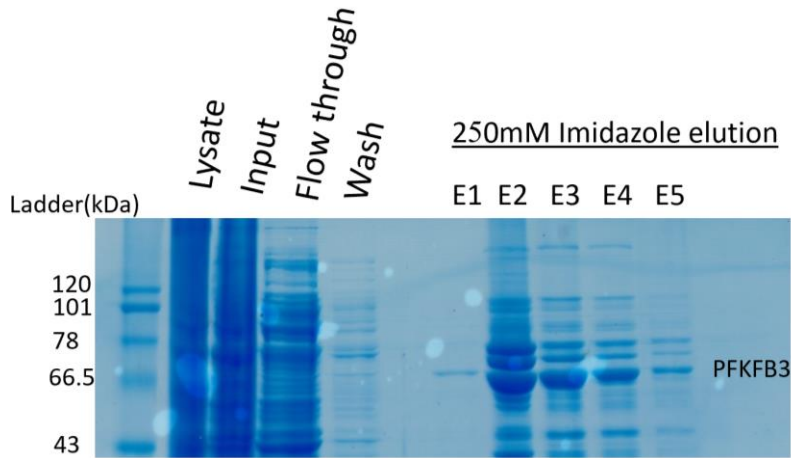
Figure 6: Purification of His-PFKFB3.
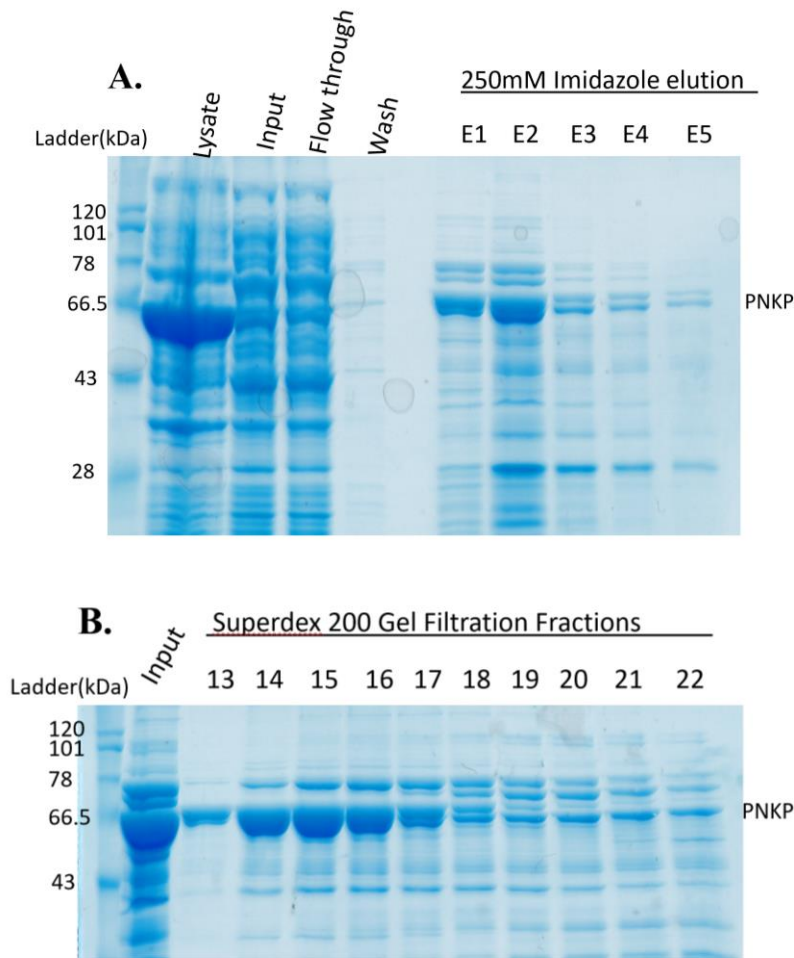
Figure 7: Purification of His-PNKP with (A) Nickle step and (B) size-exclusion step.

Fru-2,6-P$_2$ interacts with PNKP and enhances its activity

To study the interaction between PNKP and Fru-2,6-P$_2$ I produced Fru-2,6-P$_2$ using a biosynthetic route using purified PFKFB3, F6P, and ATP. To purify Fru-2,6-P$_2$, I first followed the methods used by *Myers et al.* which passes diluted reaction mixture through Q Sepharose Fast Flow beads and step-elutes Fru-2,6-P$_2$ out at 350mM TEABC pH8.5 (Myers et al., 2010). The 350mM fraction I obtained was dried by SpeedVac and sent for the MS analysis. The MS data showed a peak at the molecular weight of 340, indicating the presence of Fru-2,6-P$_2$. Since the Fru-2,6-P$_2$ we purified contains ADP and ATP, we also prepared the same reaction without adding PFKFB3, and purify it with the same method. The eluted 350mM fraction is named "Mock", which contains a similar amount of ATP and possibly ADP but no Fru-2,6-P$_2$.
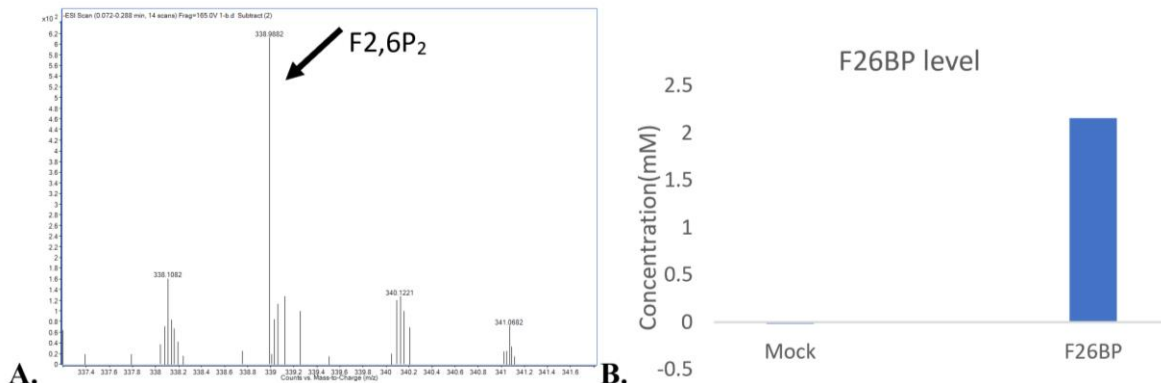
Figure 8: Production of F2,6P$_2$ and elution using the step gradient (100-350mM TEABC pH8.5). (A). The ESI-MS analysis of the presence of F2,6P$_2$ in the 350mM fraction after the elution. (B). Measurement of purified F2,6P$_2$ using the F6P assay kit.

To test the binding of Fru-2,6-P$_2$ with PNKP, we checked PNKP stability using the NanoTemper Tycho instrument to determine whether PNKP stability is altered by Fru-2,6-P$_2$ in a buffer containing 25mM Tris-HCl pH7.5, 150mM NaCl, and 5mM MgCl$_2$. NanoTemper Tycho is a quick method to qualitatively measure the effect of a ligand on a protein, but quantitative characterization is not provided by this method. The first derivative of the PNKP denaturation

curve shows two peaks at 43 and 55°C respectively, and the second peak is significantly

decreased with the presence of Fru-2,6-P₂. However, a similar effect is also observed in Mock

with a lesser extent (Figure 9A). We hypothesized that the effect we observed from the mock is

contributed by ATP. To validate our hypothesis, I checked the PNKP stability with ATP and

found a similar effect on PNKP, and we purposed that the ATP contributes to the change in

PNKP stability we observed on Fru-2,6-P₂ purified from the batch (Figure 9B). Therefore, we

need to further purify Fru-2,6-P₂ to separate it from ATP in order to quantitatively characterize its

binding to PNKP.

A.

B.
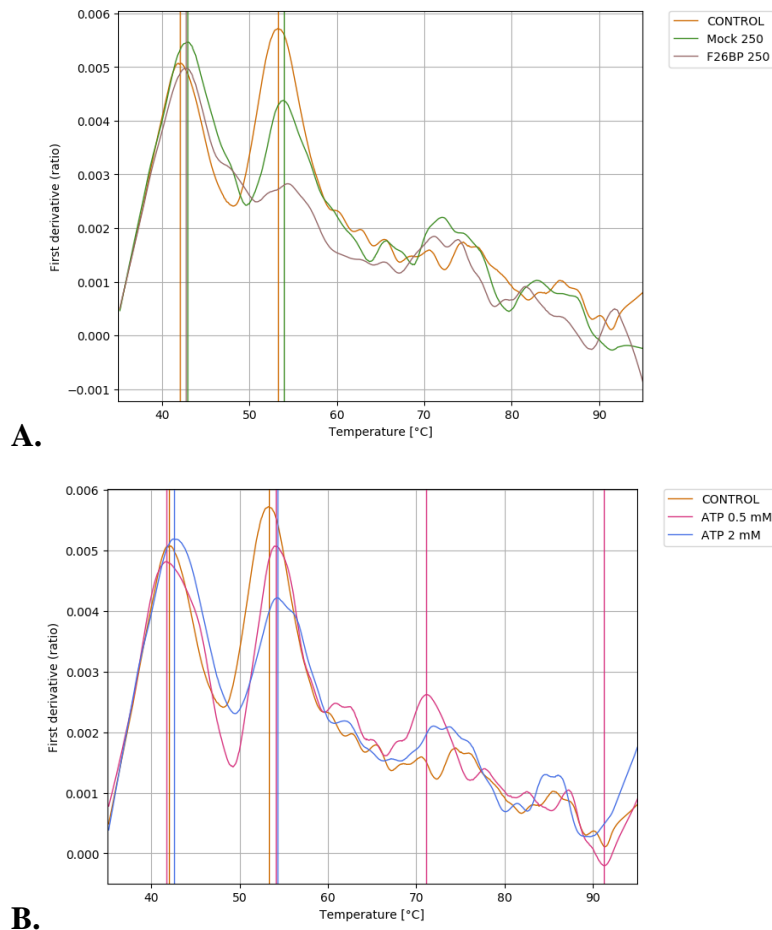
Figure 9: PNKP stability change with Fru-2,6-P₂, Mock, and ATP. (A). Change of PNKP
denaturation with 250μM Fru-2,6-P₂ purified from step elution or the equal amount of mock. The
change in PNKP stability is shown as the change in the first derivative of 350/330nm. (B).
Change of PNKP denaturation profile with ATP.

A. 50μM ADP + 50μM ATP:
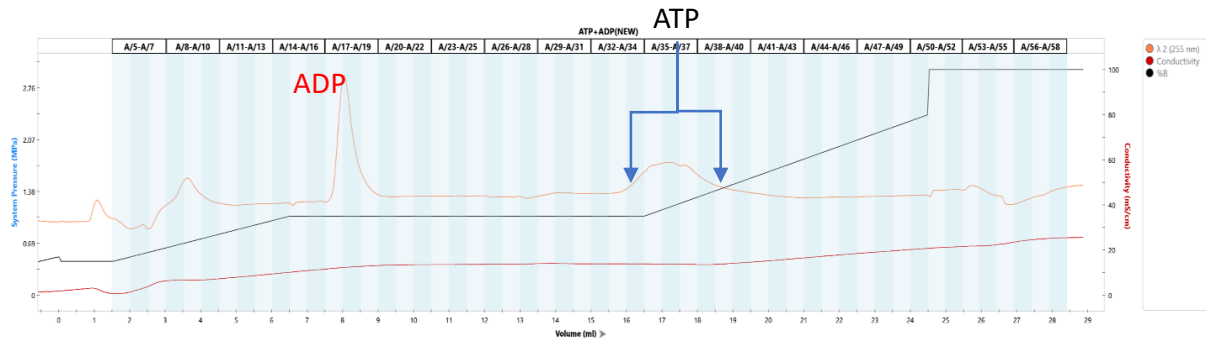
B. Fru-2,6-P$_2$ sample
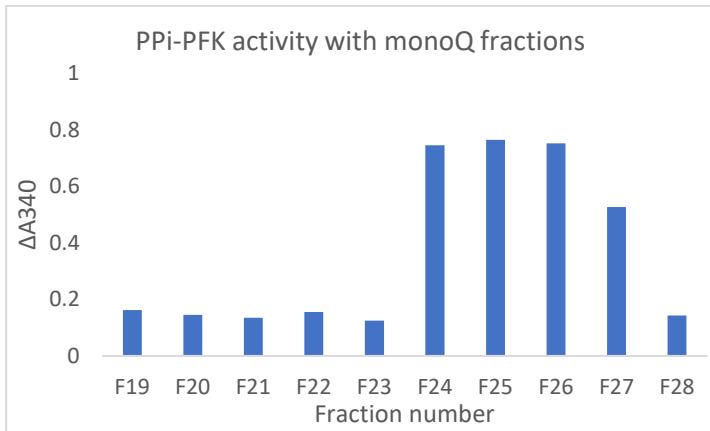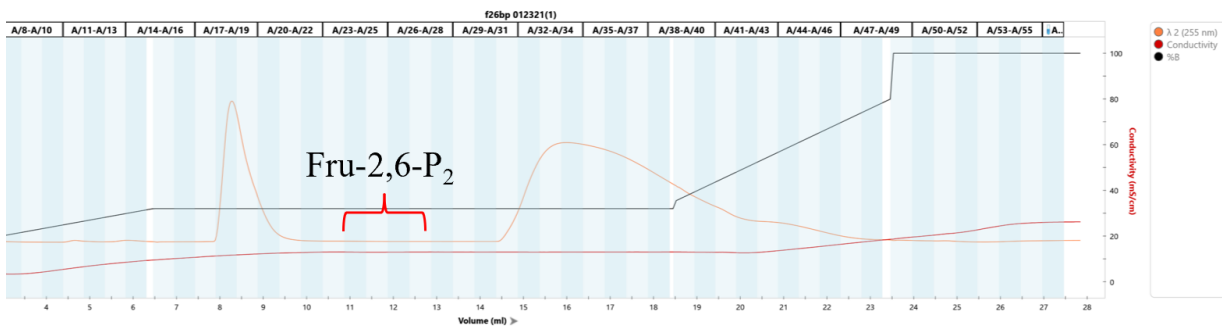
Figure 10: Detecting F2,6P$_2$ in elution gradients of MonoQ GL5/50 column. (A). Elution of ADP + ATP in mono Q column. (B). Elution profile of F2,6P$_2$ in the fraction 350mM TEABC pH8.5 and (C) F2,6P$_2$ in each fraction was detected using the PPi-PFK assay and the presence of F2,6P$_2$ is indicated with the increase in ΔA_{340}.

To get purified Fru-2,6-P_2 free from ADP or ATP, I performed secondary purification using the MonoQ GL5/50 column. To determine whether Fru-2,6-P_2 can be separated from ADP and ATP with gradient elution method, I firstly passed 50µM ATP and ADP to determine the peaks that ATP and ADP are eluted (Figure 10A). Next, I passed purified Fru-2,6-P_2 through the MonoQ column and tested the presence of Fru-2,6-P_2 in each elution fraction using the PPi-PFK assay. It is necessary to assay every fraction since Fru-2,6-P_2 does not absorb light unlike ATP and ADP. Pyrophosphate-dependent phosphofructokinase (PPi-PFK) is an enzyme in plants that converts F6P to F1,6P_2 using pyrophosphates and it is activated by Fru-2,6-P_2. PPi-PFK assay measures increase in the conversion of F6P to F16BP by PPi-PFK with the presence of Fru-2,6-P_2. At a nanomole scale, the increase in the production of F16BP is linearly correlated with the concentration of Fru-2,6-P_2 (Schaftingen at al., 1982). The PPi-PFK assay showed that Fru-2,6-P_2 is eluted between following ADP but preceding ATP elution (Figure 10B-C). However, the amount of Fru-2,6-P_2 we obtained from the MonoQ column was too low that we couldn't use it to detect the effect of Fru-2,6-P_2 on PNKP. To obtain a higher amount of Fru-2,6-P_2, I performed one-step purification of Fru-2,6-P_2 with Q Sepharose Fast Flow using the gradient elution. After the Fru-2,6-P_2 enzymatic reaction, I added glucose to 2mM with 1U hexokinase and incubated the mixture for 5 minutes before quenching the reaction to remove excess ATP. Next, I directly loaded the reaction mixture in a 5mL prepacked Q Sepharose Fast Flow column and eluted the fractions using the optimized gradient. With the newly optimized method, we successfully separated Fru-2,6-P_2 from ADP and ATP (Figure 11A).

A.

B.

Substrate(nM)	50	50	50	50	50	50	50	50	50	50
PNKP(pg/uL)		2	2	2	2	2	2	2	2	2
Elution fractions			18	19	20	40	41	42	43	44

(TAMRA)

3'-OH

3'-P
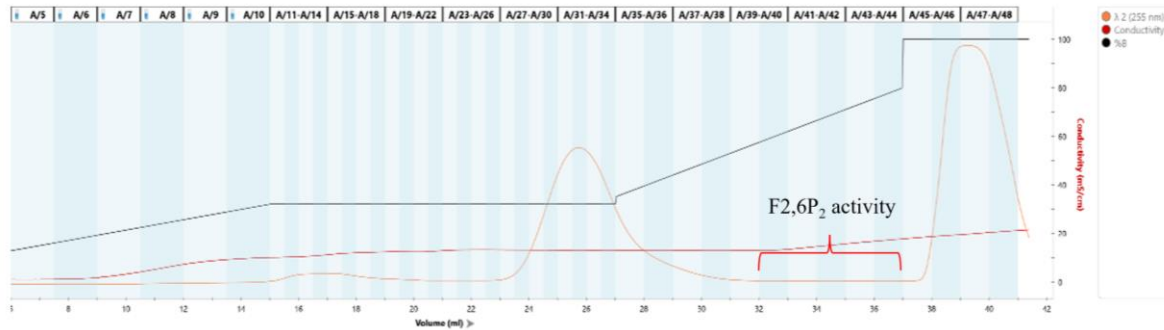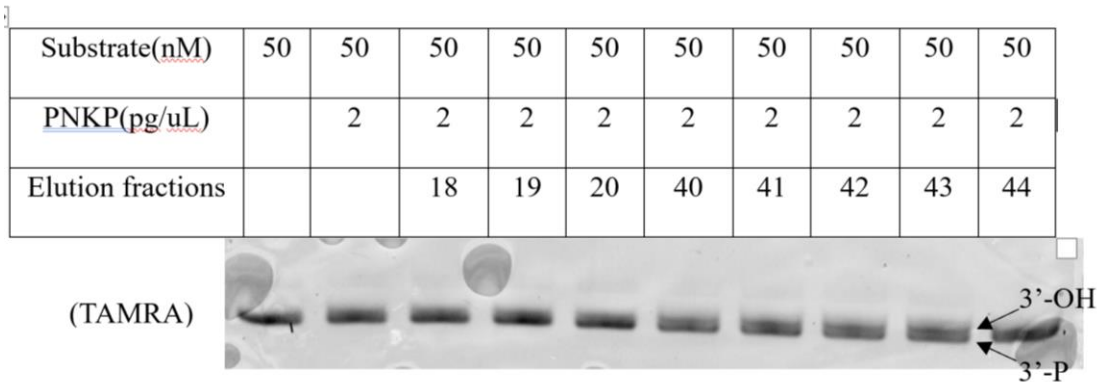
Figure 11: PNKP phosphatase assay on fractions containing Fru-2,6-P$_2$. (A) Fru-2,6-P$_2$ was purified using the prepacked Q Sepharose Fast Flow column and eluted with the gradient. Fractions containing Fru-2,6-P$_2$ (40-44) are indicated. (B)100μL Fractions containing Fru-2,6-P$_2$ and three control fractions (18-20) were dried and their effect on PNKP phosphatase activity is tested using the PNKP phosphatase assay. Bands representing 3'-OH and 3'-P are indicated.

Our collaborator used the ^{32}P-labeled phosphatase assay to show PNKP activity, and we tried to use an alternative method to study how PNKP activity is affected by Fru-2,6-P$_2$. I performed a PNKP biochemical activity assay using the fluorescent-labeled oligos. I tested PNKP activity with fractions containing only Fru-2,6-P$_2$ and found that PNKP phosphatase activity is enhanced by fractions containing purified Fru-2,6-P$_2$, which is consistent with our collaborator's result (Figure 11B).

Next, I used the purified Fru-2,6-P$_2$ to characterize its effect on PNKP using NanoTemper Tycho. I measured the amount of purified Fru-2,6-P$_2$ using the PPi-PFK assay and examined its binding to PNKP. PNKP denaturation profile also showed that pure Fru-2,6-P$_2$ alters the thermal stability of PNKP. The addition of Fru-2,6-P$_2$ decreased the second peak in a dose-dependent manner and is saturated after 75μM (Figure 12). To quantitatively characterize the binding of Fru-2,6-P$_2$ to PNKP, I performed the microscale thermophoresis (MST) assay on PNKP with Fru-2,6-P$_2$. The MST assay shows that Fru-2,6-P$_2$ interacts with PNKP with an affinity of 19.1±3.8μM (Figure 13). Together, my results suggest that Fru-2,6-P$_2$ directly binds to PNKP and activates it phosphatase activity.

Altogether, I was able to prepare and purify Fru-2,6-P$_2$ and confirmed its binding to PNKP in vitro. Work done by our collaborator's lab further confirmed that pure Fru-2,6-P$_2$ was able to rescue PNKP loss of activity in cells devoid of PFKFB3.
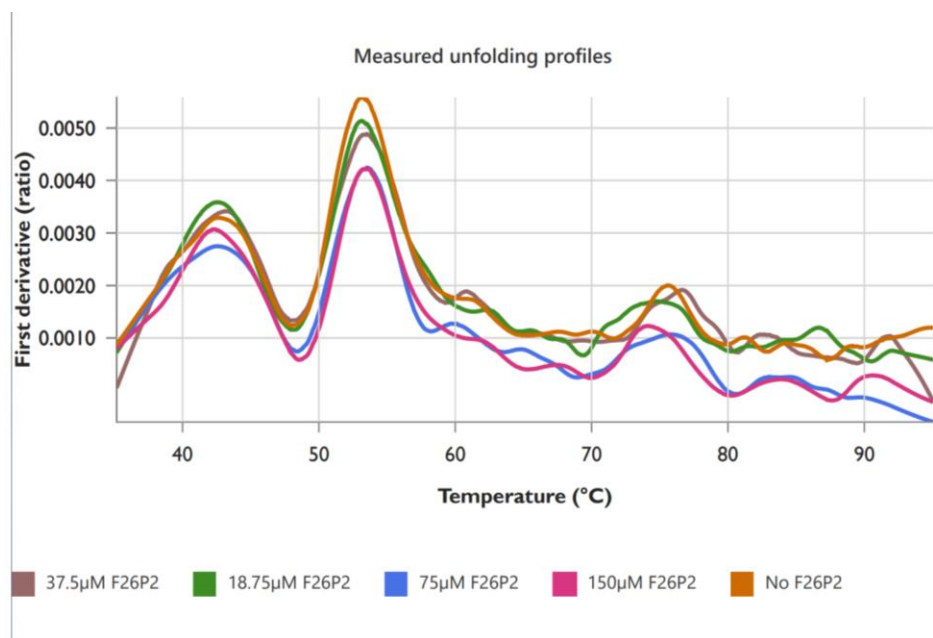
Figure 12: Effect of the pure Fru-2,6-P$_2$ fraction dilutions on PNKP stability.
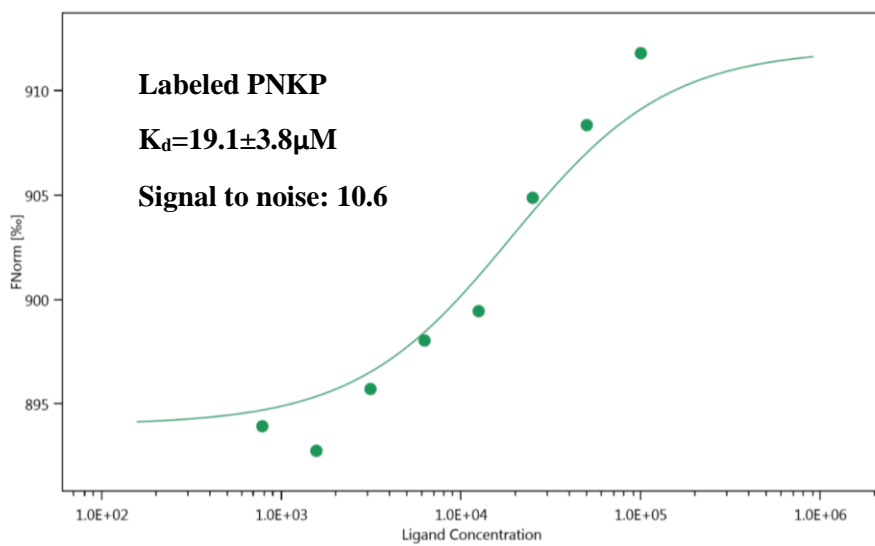
Figure 13: Data analysis of the microscale thermophoresis of PNKP with Fru-2,6-P₂. MST-determined binding affinity is shown.
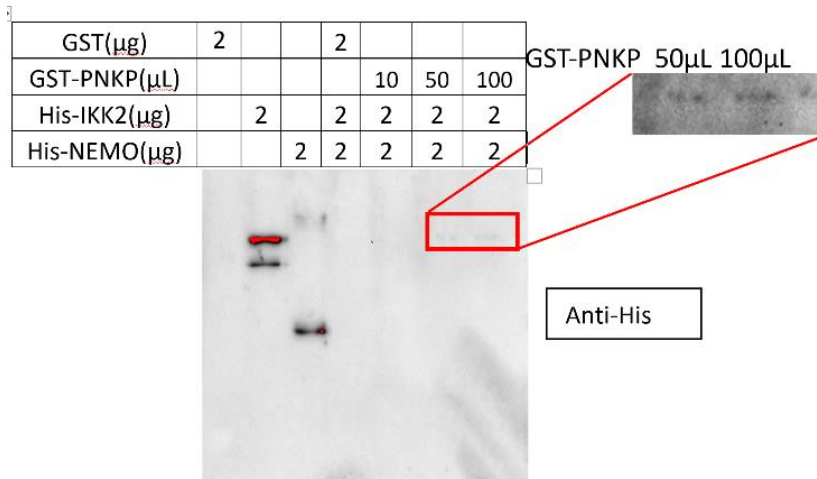
Figure 14: Western blot showing that IKK2 weakly binds to PNKP.
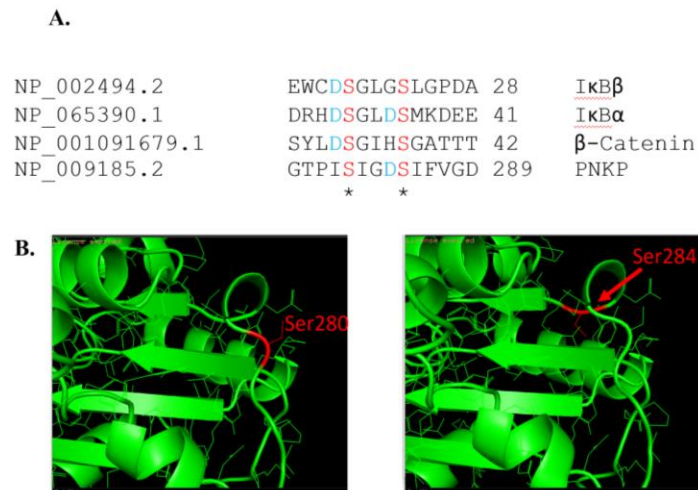
Figure 15: **Sequence homology between the known IKK2 substrates and PNKP** (A) and serine 280 and 284 in the crystal structure of murine PNKP showing that S284 is buried in the interface.

Characterizing IKK2 in vitro phosphorylation on PNKP

We are interested in whether IKK2 plays a role in regulating PNKP. The in vitro pull-down assay shows that IKK2 weakly binds to PNKP (Figure 14). Since IKK2 is a kinase and it phosphorylates many proteins other than IκB proteins, we hypothesized that PNKP might be a substrate of IKK2. To validate our hypothesis, I ran the in vitro kinase assay with PNKP and IKK2 and found that IKK2 phosphorylates PNKP in vitro (Figure 16).

+IKK2(100ng)				
GST-IκBα(1-54)AA	GST-IκBα (1-54) α			PNKP (WT)
1μg	1μg	2μg		2μg

IKK2

PNKP

IκBα
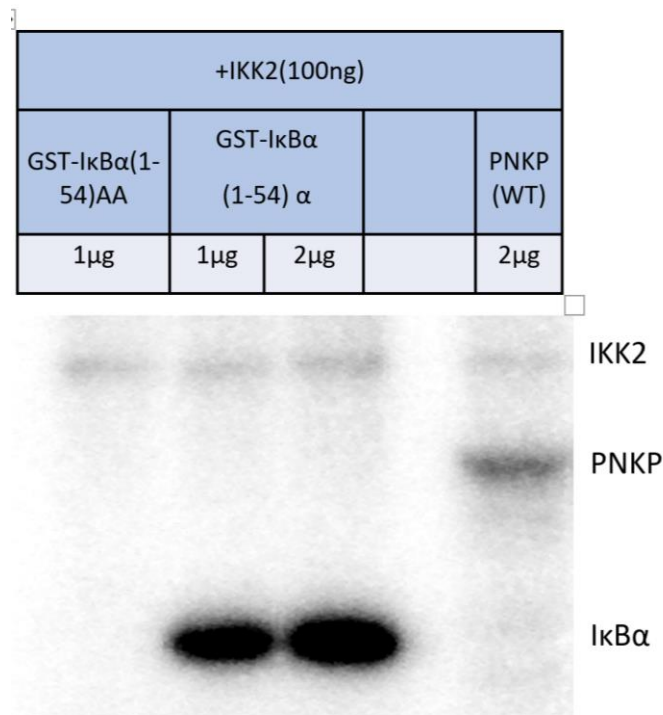
Figure 16: **^{32}P-ATP in vitro kinase assay** using 100 ng IKK2 with 1 μg of recombinant GST-IκBα(1-54)^{AA}, 1 or 2 μg of IκBα(1-54)^{α}, and 2μg of wild-type PNKP.

To determine which site of PNKP is phosphorylated, we first read the sequence to find the potential IKK2 phosphorylation motif. We identified Serine 280 and 284 as possible IKK2 phosphorylation sites since the two serine residues with three amino acids in between are also found in other motifs such as the IKK2 phosphorylation motif on IκBα (Figure 3; Figure 15A).

However, the crystal structure of murine PNKP shows that Ser284 is contained in a β sheet and is buried in the interface, which in principle should be the residue difficult to contact IKK2 resulting in less phosphorylation of this residue. Furthermore, if the phosphorylation occurs, phosphorylated Ser284 should disrupt the local folding of PNKP (Coquelle et al., 2011). In contrast, Ser280 is exposed and can be easily recognized by IKK2 or other kinases. To examine whether Ser 280 and Ser284 are the IKK2 phosphorylation sites or not, we mutated Ser280 to glutamate (S280E), Ser284 to glutamic acid (S284E), and both to glutamate (S280E/S284E, or EE) to construct the phospho-mimetic PNKP. The kinase assay on all three mutants shows low phosphorylation by IKK2 (Figure 17). This result strongly suggests that Ser280 and Ser284 are the phosphorylation sites of IKK2.
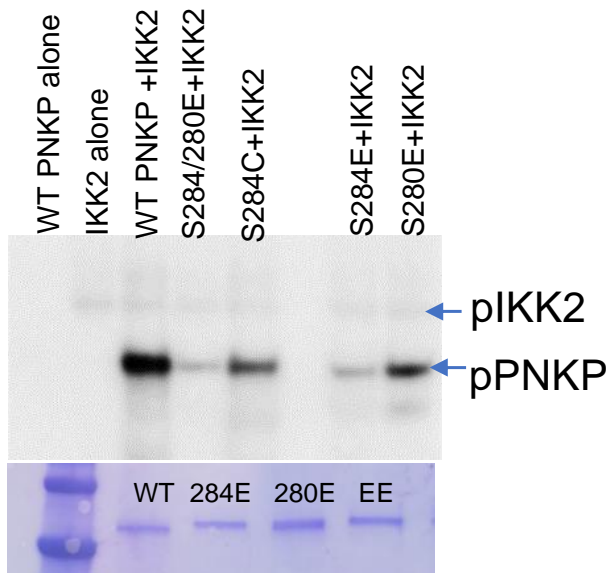
Figure 17: In vitro kinase assay showing phosphorylation of wt and PNKP mutants (Top). Protein quality and relative amounts are shown (Bottom).

To further characterize the phosphorylation of PNKP by IKK2 in vitro, we made PNKP S280A, S284C, and PNKP EC (S280E, S284C) to further study possible phosphorylation on these sites. Interestingly, both PNKP S280A and S280C show a similar level of phosphorylation

36

by IKK2 (Figure 18). However, when both sites are mutated to other residues (S280E, S284C), the phosphorylation is abrogated (Figure 18). Moreover, mutating Ser284 to cysteine, an isosteric amino acid that cannot be phosphorylated, shows slightly less phosphorylation by IKK2 compared with WT (Figure 17; Figure 18). These results further indicate that both Ser280 and Ser284 can be phosphorylated by IKK2.
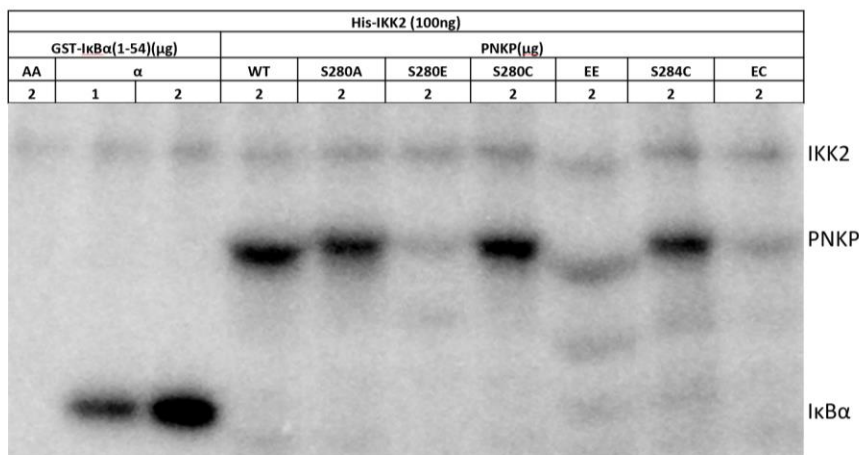
Figure 18: ^{32}P-ATP in vitro kinase assay on S280A, S280C, and EC, comparing with other mutants.

To characterize the effect of phosphorylation on PNKP activity, Both I and my collaborators tested phosphatase activity on PNKP mutants. My fluorescent-based phosphatase assay shows that the phosphatase activity of PNKP S284E is severely abrogated compared with WT. Using my PNKP S284E mutant, our collaborators observed the same effect (Figure 19A, D). Interestingly, my collaborator showed that S280E has higher phosphatase activity than WT, indicating that phosphorylation on S280 enhances PNKP activity, while phosphorylation on Ser284 or both sites arrogated PNKP activity (Figure 19A-B). Furthermore, the phosphatase activity of PNKP S284 mutants is all abrogated except the isosteric cysteine mutant (S284C),

indicating that Ser284 is important to maintain the structural integrity of PNKP (Figure 19A-B). Given that Ser284 is buried in the interface while Ser280 is exposed, it is possible that phosphorylation on Ser280 plays a predominant role and activates PNKP activity at low IKK2 activity, while excess IKK2 activity induced by factors such as chronic inflammation can cause phosphorylation on PNKP Ser284, which kills its activity. Also, the addition of Fru-2,6-P_2 restores the phosphatase activity of S284E in a dose-dependent manner (Figure 19C). This result indicates that Fru-2,6-P_2 may participate in restoring the phosphatase activity of pS284 PNKP. Together these results suggests that IKK2 is a potential regulator of PNKP, and its cellular activity may cause dramatic changes in PNKP activity.

I acknowledge Dr. Anirban Chakraborty for contributing the ^{32}P-based phosphatase assay in Figure 19 and the in vitro kinase assay in Figure 17.
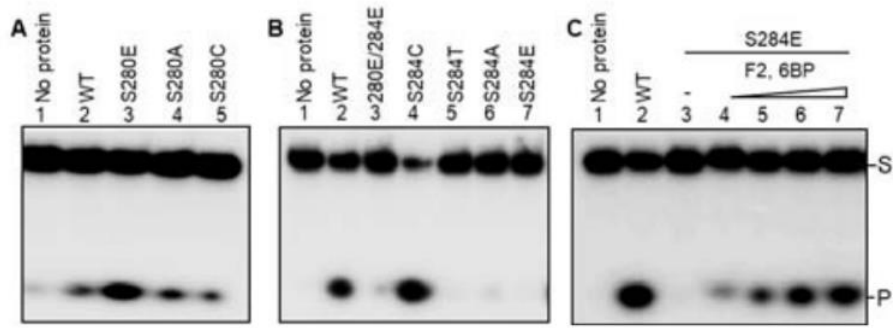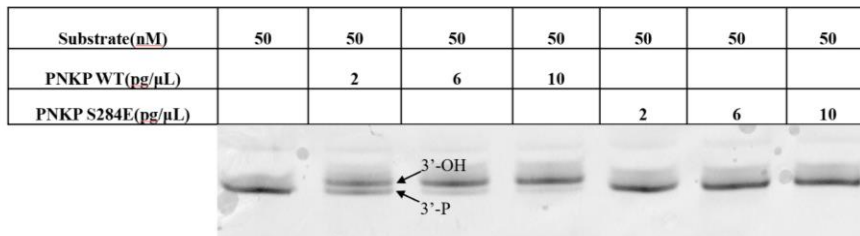
Figure 19: ^{32}P-based phosphatase activity of WT and PNKP S280 mutants (A) or S284 mutants (B) and the effect of Fru-2,6-P$_2$ on PNKP S284E. (A). Lane 1: substrates only. Ln 2-5: phosphatase activity with 1ng purified protein. (B). Ln 1: substrates only. Ln 2-7: phosphatase activity with 1ng purified protein. (C). Phosphatase activity of 1ng WT (lane 2) and S284E with different concentration (25-100μM) of Fru-2,6-P$_2$ (lane 3-7). (D). Fluorescence-based phosphatase activity of PNKP WT and S284E.

Table 1: List of Control and SCA3 samples.

Sample ID	Classification	Tissue Type	Nuclear [F26P2](pmol/mg wet tissue)
57	Control	Frontal Cortex	4.167
409	Control	Frontal Cortex	1.236
619	Control	Frontal Cortex	3.391
1073	Control	Frontal Cortex	4.167
1602	SCA3	Frontal Cortex	1.356
1549	SCA3	Frontal Cortex	2.046
1832	SCA3	Frontal Cortex	0.425
1930	SCA3	Frontal Cortex	1.667
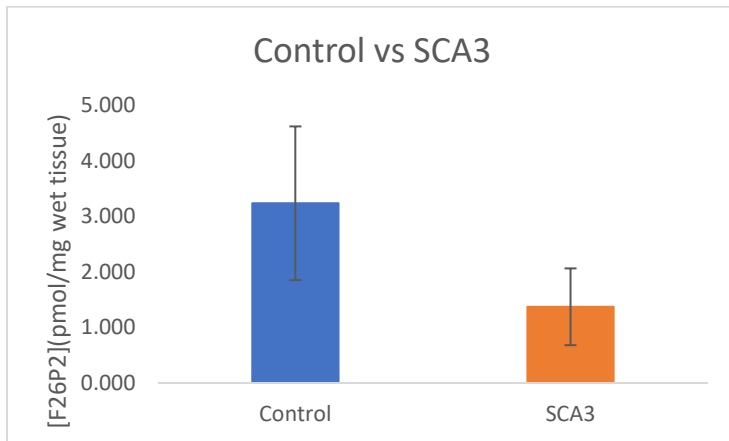
Figure 20: Level of Fru-2,6-P_2 in nuclear extracts of Control and SCA3 patient frontal cortexes.

Table 2: List of Control and HD patients.

Sample ID	Age	Sex	PMI hrs	Classification	Tissue type	PNKP activity	Nuclear [F26P2] (pmole/mg wet tissue)
14	65	M	24	Control	Frontal cortex	Robust	1.859
609	61	M	24	Control	Frontal cortex	Medium	1.046
729	59	M	12	Control	Frontal cortex	Robust	0.965
260	39	M	NR	Control	Frontal cortex	Robust	1.588
915	81	M	14	Control	Frontal cortex	Robust	1.425
283	70	M	21	Control	Frontal cortex	Robust	1.778
1174	54	M	7	HD	Frontal cortex	Abrogated	1.236
761	76	M	16	HD	Frontal cortex	Abrogated	0.179
1017	65	M	12	HD	Frontal cortex	Abrogated	0.125
1122	70	M	8	HD	Frontal cortex	partially abrogated	1.154
1333	58	M	19	HD	Frontal cortex	Abrogated	0.802
927	53	M	22	HD	Frontal cortex	Abrogated	0.748
423	41	M	7	HD	Frontal cortex	Abrogated	1.534
57	74	F	6	Control	Frontal Cortex	Robust	0.775
110	73	F	14	Control	Frontal Cortex	medium	0.965
1539	53	F	11	Control	Frontal Cortex	Robust	0.531
1459	72	F	10	HD	Frontal Cortex	Abrogated	0.287
2241	68	F	25	HD	Frontal Cortex	Abrogated	0.667
1232	61	F	6	HD	Frontal Cortex	Abrogated	0.260
1298	49	F	13	HD	Frontal Cortex	Abrogated	0.504
1071	44	F	7	HD	Frontal Cortex	Abrogated	0.125
644	45	M	22	Control	Frontal cortex	Faint	1.154
172	70	M	15	Control	Frontal cortex	Medium	1.696
718	83	M	28	Control	Frontal cortex	not checked	1.615

Table 2: List of Control and HD patients. (Continued)

1874	71	M	4	Control	Frontal cortex	Not detected	0.775
675	43	M	21	Control	Frontal cortex	Medium	1.398
1024	68	M	5	HD	Frontal cortex	Partially abrogated	0.504
565	58	M	8	HD	Frontal cortex	Not abrogated	1.127
1876	71	M	7	HD	Frontal cortex	Not abrogated	1.561
52	81	M	17	HD	Frontal cortex	Not abrogated	1.967
383	43	M	NR	HD	Frontal cortex	Not abrogated	1.290
115	62	M	9	HD	Frontal cortex	Abrogated	1.371
899	76	F	14	Control	Frontal cortex	Not detected	1.724
409	48	F	5	Control	Frontal cortex	Not detected	1.669
892	69	F	16	Control	Frontal cortex	Minute activity	1.588
1508	56	F	NR	HD	Frontal cortex	Abrogated	0.748
107	76	F	8	HD	Frontal cortex	Abrogated	0.938
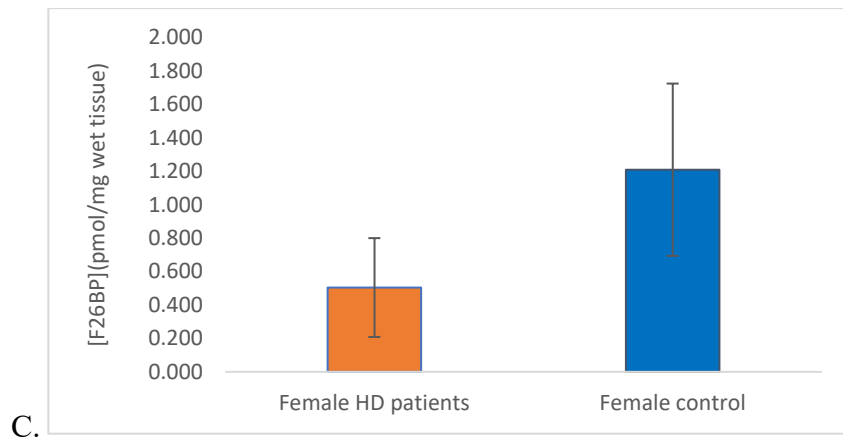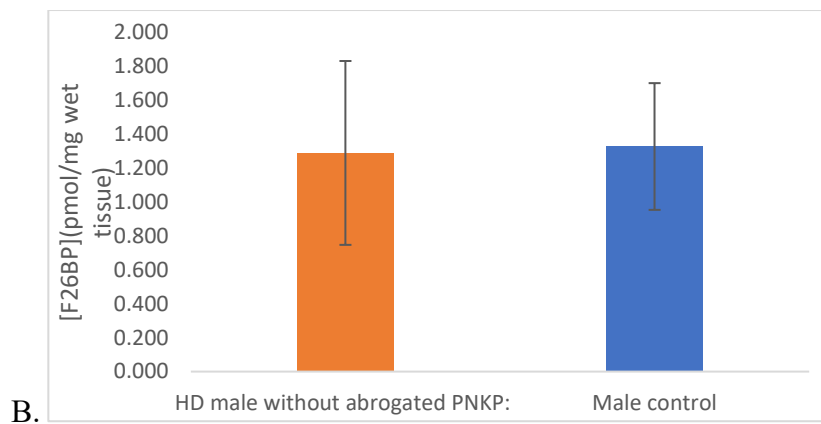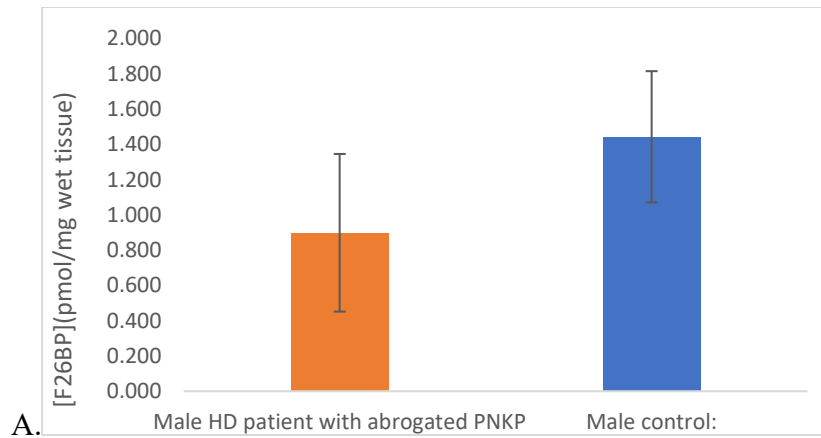
Figure 21: Fru-2,6-P₂ level in the nuclear extracts of control and HD patients. (A). Fru-2,6-P$_2$ level in male control and HD with abrogated PNKP activity. (B). Fru-2,6-P$_2$ level in the male control and HD without abrogated PNKP activity. (C). Fru-2,6-P$_2$ level in female control and HD with abrogated PNKP activity.

Measurement of Patient Nuclear Fru-2,6-P$_2$

The discovery that PFKFB3 and Fru-2,6-P$_2$ is involved in PNKP associated DNA repair complex motivated us to find if abrogated Fru-2,6-P$_2$ level is associated with neurological diseases. Both SCA3 and HD are neurodegenerative diseases with mutant proteins containing expanded polyglutamine-rich regions. Our collaborators have established that ATXN3 binds to PNKP and stimulates its activity, while mutant ATXN3 abrogates PNKP activity instead, which causes accumulation of DNA damage and SCA3 pathology (Chatterjee et al., 2015; Chakraborty et al., 2020). Since the PNKP activities in SCA3 and HD patients are low, we are interested in if the nuclear Fru-2,6-P$_2$ level in patient brains are altered. Therefore, we aimed to determine the level of nuclear Fru-2,6-P$_2$ in SCA3 and HD patients. We obtained four control and four SCA3 patients' brain postmortem samples, and I measured the nuclear Fru-2,6-P$_2$ level in the Control and SCA3 samples. The result shows that level of nuclear Fru-2,6-P$_2$ in the SCA3 patient cortexes is approximately 50% lower comparing with control (Figure 20). The result indicates that the reduced level of nuclear Fru-2,6-P$_2$ is potentially a factor in the SCA3 pathology.

For the HD sample, our collaborators tested PNKP activity on 21 HD patients and found that 17 of them had abrogated PNKP activity (Table 2). I tested all control and HD samples and found that the level of nuclear Fru-2,6-P$_2$ in male HD patients with abrogated PNKP is significantly lower than the level in control, while the nuclear Fru-2,6-P$_2$ level in male HD patients without abrogated PNKP activity is close to the level of control (Figure 21A-B). For the female samples, female HD patients showed abrogated PNKP activity, which might be caused by a smaller number of patients tested. We found that females have a slightly a lower level of nuclear Fru-2,6-P$_2$ compared with males, and female HD patients also have lower level of nuclear Fru-2,6-P$_2$ compared with female control (Figure 21C). Together, our results suggested

44

that there is a strong correlation between the level of PNKP activity and nuclear Fru-2,6-P$_2$ level

in brains, and lack of nuclear Fru-2,6-P$_2$ is potentially a factor of neurodegenerative diseases

such as SCA3 and HD.

IV: Discussion

Although PFKFB3 is extensively studied for its role in cancer, most of the studies, however, focus on how PFKFB3 is regulated, while its product, Fru-2,6-P_2, is rarely studied. This is largely due to the stereotype that Fru-2,6-P_2 is an important regulator of PFK-1, which makes its role beyond glycolysis less likely. Since the major function of PFKFB3 is producing Fru-2,6-P_2, the function of PFKFB3 in cells is closely related to Fru-2,6-P_2. Though previous studies on the role of PFKFB3 in the homologous recombination pathway suggested that the kinase activity of PFKFB3 is required for its role in the homologous recombination, the author did not dig into how Fru-2,6-P_2 plays a role in the process and studied the role of PFKFB3 as a scaffold-protein-like function instead (Gustafsson et al., 2018).

My goals are to determine whether Fru-2,6-P_2 regulates PNKP phosphatase activity and whether IKK2 is a possible regulator of PNKP. In the first part of my thesis, I produced and purified F-2,6-P_2 in vitro using the combination of enzymatic production and anion exchange chromatography and quantified my purified product using the enzymatic assay. I showed that Fru-2,6-P_2 directly binds to PNKP through microscale thermophoresis. To our knowledge, this is the first time that Fru-2,6-P_2 is shown directly binding to proteins other than PFK-1, and the second role of PFKFB3 in the nucleus besides its function in regulating cell cycles. Combined with the role of PFFKB3 in homologous recombination, we established that PFKFB3 is a critical enzyme in DNA DDSR. Besides my in vitro studies, I also shipped my purified Fru-2,6-P_2 to my collaborators, who performed in vivo studies. They showed that Fru-2,6-P_2 enhances PNKP activity in vivo, which rescues the DNA repair in siPFKFB3 cells.

In the second part of my thesis, I established that IKK2 phosphorylates PNKP in vitro, and the phosphorylation sites are likely to be Ser280 and Ser284. Interestingly, phosphorylation on either site has a distinct effect on its phosphatase activity. However, whether the IKK2

47

phosphorylates PNKP in vivo is yet to be known. The in vivo study is limited due to the different localization of two proteins. While PNKP is a nuclear protein, IKK2 locates in the cytoplasm. While papers are reporting that IKK2 presents the nucleus in different conditions such as UV-induced NF-κB activation, the mechanism of how IKK2 enters the nucleus remains a challenging question (Ear et al., 2005, Tsuchiya et al., 2010). Therefore, more in vivo experiments need to be performed to determine the relation between IKK2 and PNKP. Since UV-irradiation induces DNA damage with 3'-phosphate, one possible hypothesis is that IKK2 enters the nucleus upon UV irradiation and phosphorylates PNKP, which regulates its activity. The most intriguing aspect of PNKP phosphorylation is that whereas the phosphorylation at S280 enhances 3'-phosphatase activity, phosphorylation at S284 completely abrogates its phosphatase activity. It is being speculated that S280 phosphorylation maintains homeostatic function of PNKP which is to correct DNA damages in basal state to maintain the genome stability when IKK2 activity is low. On the contrary, Ser284 phosphorylation is the death signal. That is, when this serine is phosphorylated, the cell cannot survive because of excessive DNA breaks. Perhaps, this occurs when cells are under excessive oxidative stress when IKK2 activity is maximum. More studies are needed to confirm or reject the model.

The discovery that PFKFB3 is a component of the DNA strand break repair complex, prompted us to speculate that Fru-2,6-P_2 might play a role in DNA repair. Having established that Fru-2,6-P_2 binds and activates PNKP and that PNKP activity in the brains of HD and SCA-3 patients was low, we wanted to measure Fru-2,6-P_2 levels in the brain extracts. I tested the Fru-2,6-P_2 level in spinocerebellar ataxia 3 (SCA3) patients and found a decreased level of nuclear Fru-2,6-P_2 compared with control samples. Moreover, I tested Fru-2,6-P_2 concentration in Huntington's Disease (HD) patients and found that those HD patients with low PNKP activity in

their brain also contained lower Fru-2,6-P_2 levels. Our collaborators have found that in all samples where Fru-2,6-P_2 levels are low, PFKFB3 levels are also low. In the case of HD, about 70% of patients exhibited low PFKFB3 and low levels of Fru-2,6-P_2. These results suggest that PFKFB3 might play an important role in neurodegenerative diseases. It's noticeable that the binding affinity we obtained from the in vitro MST assay is significantly lower than the concentration of Fru-2,6-P_2 we obtained from the nuclear extracts of cortex samples, suggesting that the interaction between PFKFB3 and PNKP might be necessary for enhancing PNKP activity. It is also possible that in the presence of entire repair complex, the affinity of Fru-2,6-P_2 for PNKP becomes higher. It is also possible that Fru-2,6-P_2 works in conjunction with another ligand and the affinity is much higher when the other ligand is present.

There are still several important but unanswered questions that need attention: The cause of neurodegeneration in the other ~30% of HD patients where PFKFB3 and Fru-2,6-P_2 levels are normal needs to be determined. Although we found Fru-2,6-P_2 levels are low in SCA-3 samples we tested, we tested only four samples due to the rarity of the disease. More SCA-3 samples should be tested to conclusively suggest the fraction of SCA-3 patients affected due to low PFKFB3/ Fru-2,6-P_2. Another aspect to be investigated is the role of PFKFB3 in other neurological diseases such as Alzheimer's disease, Parkinson's disease. Finally, it is intriguing to think if its analogs can be used as therapy in cases where low levels of Fru-2,6-P_2 are linked to the pathology.

References

Madabushi, R., Pan, L., Tsai, L. "DNA Damage and its Links to Neurodegeneration." *Neuron.* Vol. 83,2 (2014): 266-282.

Bender, A., Krishnan, K.J., Morris, C.M., Taylor, G.A., Reeve, A.K., Perry, R.H., Jaros, E., Hersheson, J.S., Betts, J., Klopstock, T., Taylor, R.W., Turnbull, D.M. "High levels of mitochondrial DNA deletions in substantia nigra neurons in aging and Parkinson disease." *Nature Genetics.* 38 (2006): 515-517.

Mullaart, E., Boerrigter, M.E.T.I., Ravid, R., Swaab, D.F., Vijg, J. "Increased levels of DNA breaks in cerebral cortex of Alzheimer's disease patients." *Neurobiology of Aging.* Vol. 11,3 (1990): 169-173.

Martin, Lee J. "Neuronal cell death in nervous system development, disease, and injury (Review)." *International Journal of Molecular Medicine.* 7 (2001):455-478.

Gao, R., Chakraborty, A., Geater, C., Pradhan, S., Gordon, K.L., Snowden, J., Yuan, S., Dickey, A.S., Choudhary, S., Ashizawa, T., Ellerbey, L.M., Spada, A.R.L., Thompson, L.M., Hazra, T.K., Sarkar, P.S. "Mutant huntingtin impairs PNKP and ATXN3, disrupting DNA repair and transcription." *Elife.* (2019) 8,42988.

Chakraborty, A., Tapryal, N., Venkova, T., Mitra, J., Vasquez, V., Sarker, A.H., Duarte-Silva, S., Huai, W., Ashizawa, T., Ghosh, G., Maciel, P., Sarkar, P.S., Hedge, M.L., Chen, X., Hazra, T.K. "Deficiency in classical nonhomologous end-joining–mediated repair of transcribed genes is linked toSCA3 pathogenesis." *Proceedings of National Academy Sciences.* 117,14 (2020):8154-8165.

Jiang, H., Nucifora Jr, F.C., Ross, C.A., DeFranco, D.B. "Cell death triggered by polyglutamine-expanded huntingtin in a neuronal cell line is associated with degradation of CREB-binding protein." *Human Molecular Genetic*s. 12,1 (2003): 1-12.

Dobson, C.J. and Allinson, S.L. "The phosphatase activity of mammalian polynucleotide kinase takes precedence over its kinase activity in repair of single strand breaks." *Nucleic Acids Research*. 34 (2006), 2230– 2237.

Garces, F., Pearl L.H., Oliver, A.W. "The structural basis for substrate recognition by mammalian polynucleotide kinase 3' phosphatase." *Molecular cell.* Vol. 44,3 (2011): 385-396.

Dumitrache, L.C. and KcKinnon, P.J. "Polynucleotide kinase-phosphatase (PNKP) mutations and neurologic disease." *Mechanisms of Ageing and Development*. (Jan 161(Pt A), 2017): 121-129.

Parsons, J.L., Khoronenkova, S.V., Dianova, I.I., Ternette, N., Kessler, B.M., Datta, P.K., Dianov, G.L. "Phosphorylation of PNKP by ATM prevents its proteasomal degradation and enhances resistance to oxidative stress." *Nucleic Acids Research.* 40 (2012): 11404-11415.

Karin, M., and Y. Ben-Neriah. "Phosphorylation Meets Ubiquitination: The Control of NF-[Kappa]B Activity." *Annual Review of Immunology*. 18 (2000): 621–663.

Delhase, M., Hayakawa, M., Chen, Y. and Karin M. "Positive and negative regulation of IκB kinase activity through IKKβ subunit phosphorylation." *Science*. 284 (1999): 309-313.

Yang, F., Tang, E., Guan, K., Wang, C.Y. "IKKβ Plays an Essential Role in the Phosphorylation of RelA/p65 on Serine 536 Induced by Lipopolysaccharide." *The journal of immunology*. Vol. 170,11 (2003): 5630-5635.

Beinke, S., Robinson, M.J., Hugunin, M., Ley, S.C. "Lipopolysaccharide Activation of the TPL-2/MEK/Extracellular Signal-Regulated Kinase Mitogen-Activated Protein Kinase Cascade Is Regulated by IκB Kinase-Induced Proteolysis of NF-κB1 p105." *Molecular and Cellular Biology*. Vol. 24,21 (2004): 9658-9667.

Hu, M., Lee, D., Xia, W., Golfman, L.S., Ou-Yang, F., Yang, J., Zou, Y., Bao, S., Hanada, N., Saso, H., Kobayashi, R., Hung, M. "IκB Kinase Promotes Tumorigenesis through Inhibition of Forkhead FOXO3a." *Cell.* 117 (2004): 225-237.

Antonia, R.J., Hagan R.S., Baldwin A.S. "Expanding the View of IKK: New Substrates and New Biology." *Trends in Cell Biology*. Vol. 31,3 (2021): 166-178.

Chariot, A. "The NF-κB-independent functions of IKK subunits in immunity and cancer." *Trends in Cell Biology*. Vol. 19,8 (2009): 404-413.

Schmid J.A. and Birbach, A. "IκB kinase β (IKKβ/IKK2/IKBKB)—A key molecule in signaling to the transcription factor NF-κB." *Cytokines & Growth Factors Reviews*. Vol. 91,2 (2008): 157-165.

Pilkis, S.J., Claus, T.H., Kurland, I.J., Lange, A.J. "6-Phosphofructo-2-kinase/fructose-2, 6-bisphosphatase: a metabolic signaling enzyme." *Annual Review of Biochemistry* 64 (1995): 799–835.

El-Maghrabi, M.R., Noto, F., Wu, N., Manes, N. "6-Phosphofructo-2-kinase/fructose-2, 6-bisphosphatase: suiting structure to need, in a family of tissue-specific enzymes." *Current Opinion in Clinical Nutrition and Metabolic care*. 4 (2001): 411–418.

Okar, D.A., Lange, A.J., Manzano, À., Navarro-Sabatè, A., Riera, L.S., Bartrons, R. "PFK-2/FBPase-2: maker and breaker of the essential biofactor fructose-2,6-bisphosphate." *Trends Biochemical Sciences*. 26 (2001):30–35.

Yalcin, A., Clem, B.F., Simmons, A., Lane, A., Nelson, K., Clem A.L., Brock, E., Siow, D., Wattenburg, B., Telang, S., Chesney, J. "Nuclear targeting of 6-phosphofructo-2-kinase (PFKFB3) increases proliferation via cyclin-dependent kinases." *Journal of Biological Chemistry*. 284 (2009): 24223–24232.

Yalcin, A., Clem, B.F., Imbert-Fernandez, Y., Ozcan, S.C., Peker, S., O'Neal, J., Klarer, A.C., Clem, A.L., Telang, S., Chesney, J. "6-Phosphofructo-2-kinase (PFKFB3) promotes cell

cycle progression and suppresses apoptosis via Cdk1-mediated phosphorylation of p27." *Cell Death & Disease*. (2014) 5, 1337.

Gustafsson, N.M.S., Färnegårdh, K., Bonagas, N., Ninou, A.H., Groth, P., Wiita, E., Jönsson, M., Hallberg, K., Lehto, J., Pennisi, R., Matrinsson, J., Norström, C., Hollers, J., Schultz, J., Andersson, M., Markova, N., Marttila, P., Kim, B., Norin, M., Olin, T., Helleday, T. "Targeting PFKFB3 radiosensitizes cancer cells and suppresses homologous recombination." *Nature Communications*. (2018) 9, 3872.

Warburg, O., Wind, F., Negelein, E. "The Metabolism of Tumors in the Body." *Journal of General Physiology*. 8,6 (1927): 519-530.

Atsumi, T., Chesney, J., Metz, C., Leng, L., Donnelly, S., Makita, Z., Mitchell, R., Bucala, R. "High Expression of Inducible 6-Phosphofructo-2-Kinase/Fructose-2,6-Bisphosphatase (iPFK-2; PFKFB3) in Human Cancers." *Cancer Research*. 62 (2002): 5881-5887.

Shi, L., Pan, H., Liu, Z., Xie, J., Han, W. "Roles of PFKFB3 in Cancer." *Signal Transduction and Targeted Therapy*. (2017) 2, 17044.

Schaftingen, E.V., Lederer, B., Bartrons, R., Hers, H.G. "A Kinetic Study of Pyrophosphate: Fructose-6-Phosphate Phosphotransferase from Potato Tubers. Application to a microassay of fructose 2,6-bisphosphate." *European Journal of Biochemistry*. 129 (1982): 191-195.

Kalasova, I., Hanzlikova, H., Gupta, N., Li, Y., Altmüller, J., Reynolds, J.J., Stewart, G.S., Wollinik, B., Yigit, G., Caldecott, K.W. "Novel PNKP mutations causing defective DNA strand break repair and PARP1 hyperactivity in MCSZ." *Neurology Genetics*. (2019) 5,2 320.

Myers, R.W., Baginsky, W.F., Gattermier, D.J., Geissler, W.M., Harris, G. "Enzymatic preparation of high-specific-activity β-D-[6,60-^{3}H]fructose-2,6- bisphosphate: Application to a sensitive assay for fructose-2,6-bisphosphatase." *Analytical Biochemistry*. 406 (2010):97-104.

Coquelle, N., Havali-Shahriari, Z., Bernstein, N., Green, R., Glover, M.J.N. "Structural basis for the phosphatase activity of polynucleotide kinase/phosphatase on single- and double-stranded DNA substrates." *Proceedings of National Academy Sciences*. 108,52 (2011):21022-21027.

Chatterjee, A., Saha, S., Chakraborty, A., Silva-Fernandez, A., Mandal, S.M., Neves-Carvalho, A., Liu, Y., Pandita, R.K., Hedge, M.L., Hedge, P.M., Boldolgh, I., Ashizawa, T., Koeppen, A.H., Pandita, T.K., Maciel, P., Sarkar, P.S., Hazra, T.K. "The Role of the Mammalian DNA Endprocessing Enzyme Polynucleotide Kinase 3'- Phosphatase in Spinocerebellar Ataxia Type 3 Pathogenesis." *PLOS Genetics*. (2015) 11(1):1004749.

Ear, T., Cloutier, A., McDonald, P.P. "Constitutive nuclear expression of the I kappa B kinase complex and its activation in human neutrophils." *Journal of Immunology*. 175(3) (2005): 1834-1842.

Tsuchiya, Y., Asano, T., Nakayama, K., Kato Jr, T., Karin, M., Kamata, H. "Nuclear IKKβ Is an Adaptor Protein for IκBα Ubiquitination and Degradation in UV-Induced NF-κB Activation." *Molecular Cell*. Vol. 39,4 (2010): 570-582.